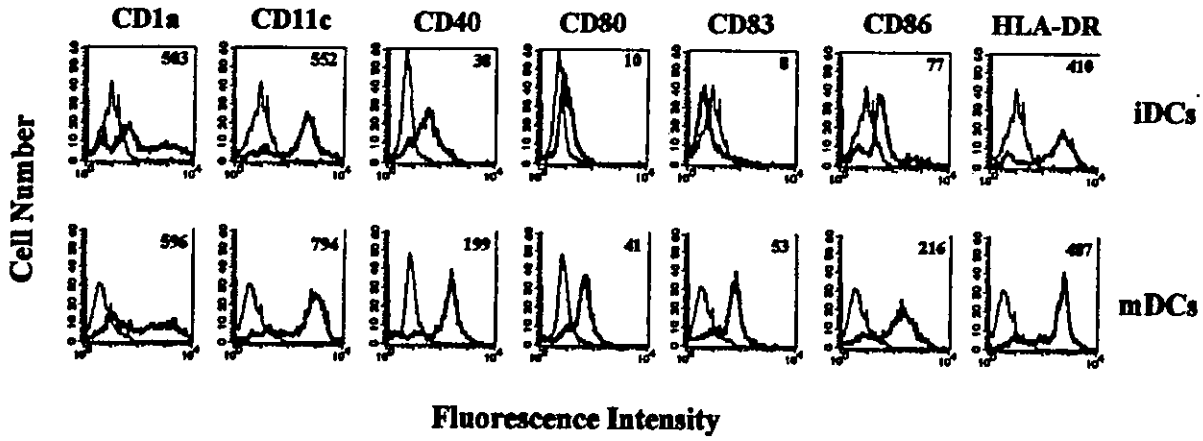

Figure 1. Surface phenotype of monocyte-derived iDCs and mDCs. DCs were labeled with the indicated FITC- and PE-conjugated mAbs (thick lines) or isotype controls (thin lines), and cell surface expression was analyzed by FACS. The histograms show the mean fluorescence intensities (MFIs). The results are representative of four experiments.

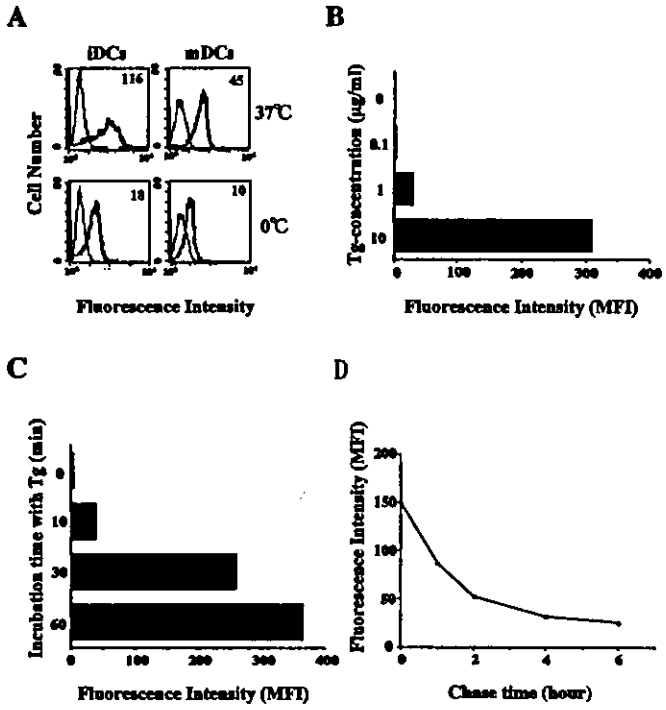

Figure 2. Endocytosis of hTg by monocyte-derived DCs. (A), iDCs and mDCs were cultured with (thick lines) or without (thin lines) FITC-labeled hTg for 30 min at 37°C or 4°C, and the internalization was assessed by flow cytometry. The values shown in the flow cytometry profiles are MFIs; the value of the background signal was <10. (B and C), iDCs were cultured with the indicated concentrations of FITC-labeled hTg for the indicated time periods at 37°C. Internalization was assessed by flow cytometry; the data are expressed as MFIs. (D), iDCs were cultured with or without FITC-labeled hTg. After a 60-min pulse at 37°C, the cells were washed and chased in the tracer-free medium for the indicated times. Internalization was assessed by flow cytometry; the data are expressed as MFIs and are representative of four individual experiments.

and IL-4 using specific ELISAs (Endogen, Woburn, MA). The sensitivity of the assays was >2 pg/ml.

Statistical analysis. Data are expressed as means ± SD. Comparisons were made using Student's t-test. Values of $p<0.05$ were considered statistically significant.

Results

Phenotypic comparison of iDCs and mDCs by flow cytometry. iDCs were preparing by incubating human PBMCs with GM-CSF plus IL-4, after which mDCs were generated by stimulating the iDCs with TNF-α. Flow cytometric analysis showed the iDCs to have a typical cell surface phenotype ($CD1a^+$, $CD11c^+$, $CD40^+$, $CD80^-$, $CD83^-$, $CD86^+$, and histocompatibility complex type II molecule human leukocyte antigen (HLA)-DR^+. Stimulation with TNF-α retained the surface expression of CD1a, CD11c and HLA-DR, and upregulate that of the co-stimulatory molecules CD80, CD86 and CD40 and the differentiation marker CD83 (Fig. 1).

The ability of monocyte-derived DCs to internalize hTg. To determine whether DCs can internalize hTg, iDCs and mDCs were cultured with FITC-labeled hTg under various conditions, and its internalization was assessed by flow cytometry. As reported previously, iDCs have high internalization activity, however, mDCs are poorly endocytic, functioning instead to present antigens to T cells (21). In fact, the ability of iDCs to internalize hTg was greater than that of mDCs (Fig. 2A), and hTg internalization by both iDCs and mDCs were diminished in the culture at 4°C. Furthermore, the uptake of FITC-labeled hTg by iDCs was dose-dependent (Fig. 2B), and maximum uptake was achieved by incubation for 60 min with 10 μg/ml hTg (Fig. 2C).

To evaluate the kinetics of hTg internalization by iDCs, incubation with FITC-labeled hTg for 60 min at 37°C was chased by incubation with tracer-free medium for the indicated times (Fig. 2D). Levels of internalize tracer declined in a chase time-dependent fashion, with 30% of the internalized FITC-labeled hTg remaining after 6 h of incubation, indicating that antigen processing occurred in iDCs.

Localization of internalized hTg within iDCs. To determine the steady-state localization of internalized hTg protein, iDCs were incubated with FITC-labeled hTg (green signal) and PE-labeled HLA-DR (red signal) and then examined under a fluorescence microscope. As shown in the left panel of Fig. 3, the HLA-DR molecules distributed mainly on marginal sites.

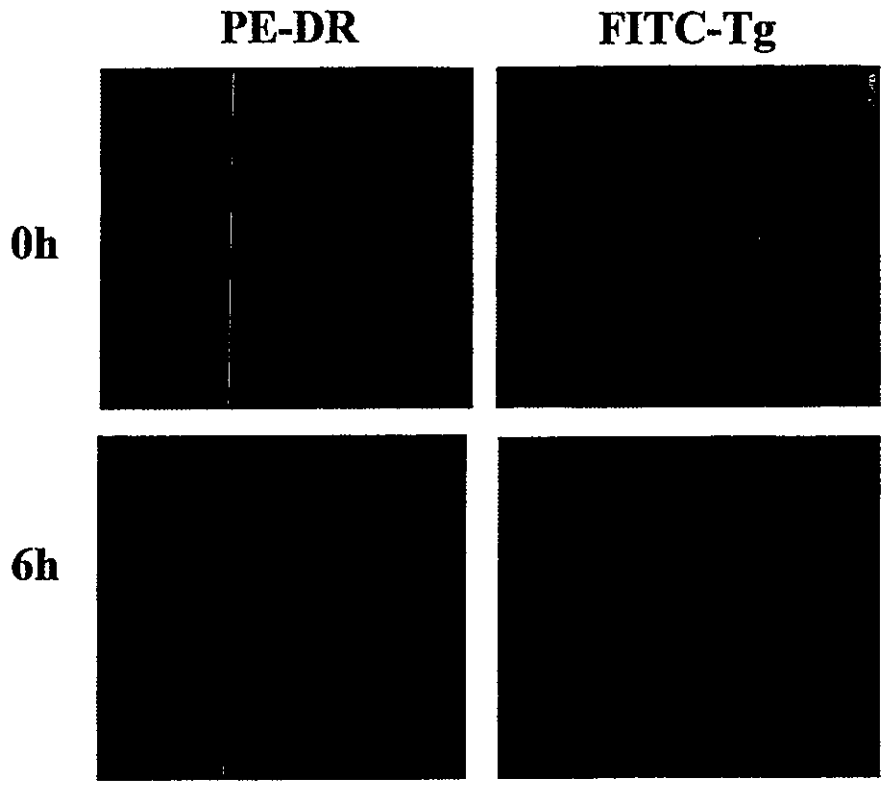

Figure 3. Cellular distribution of internalized FITC-labeled hTg within iDCs. In some cases, iDCs were incubated with FITC-labeled hTg (green) for 30 min at 37°C and then labeled with PE-conjugated HLA-DR (red) (upper panels). Alternatively, cells were cultured in tracer-free medium for 6 h at 37°C before labeling with PE-conjugated HLA-DR (lower panels). Data are representative of two individual experiments.

By contrast, FITC-labeled hTg protein accumulated mainly in the intracellular compartments and was excluded from the nucleus (Fig. 3, upper part of the right panel). After 6-h incubation with labeled antigen, the expression of HLA-DR remain on cell surface, but FITC-labeled hTg protein was concentrated at one pole of the cells, though by that time the strength for the fluorescent signal had diminished substantially (Fig. 3, lower part of the right panel). These findings indicate that FITC-labeled hTg protein is endocytosed and accumulate within structures for antigen processing.

Induction of hTg-specific T cell responses by hTg-pulsed DCs. Finally, we examined whether hTg-pulsed mDCs induce hTg-specific T cell responses. Although hTg-pulsed mDCs induced little proliferation of freshly isolated T cells (Fig. 4A), they elicited a greater response in hTg-primed T cells than was elicited by unpulsed mDCs (Fig. 4B). The hTg-primed T cell population consisted of >90% $CD4^+$ T cells (Fig. 4C), which when co-cultured with hTg-pulsed mDCs produced greater amounts of IFN-γ than when cultured alone or with unpulsed mDCs (Fig. 4D). Production of IL-4 was undetectable; apparently, hTg-pulsed mDCs selectively induce proliferation of IFN-γ-producing T cells.

Discussion

Development of new approaches to the treatment of recurred or metastatic thyroid cancers is essential to prevent the progression of disease. Several studies have showed thyroid cancer with chronic thyroiditis associated with a lower recurrence rate and improved survival rate (22,23). Furthermore, some investigators have reported that the presence of lymphocytic infiltration in papillary thyroid carcinoma is associated with a better prognosis, a lower recurrence rate, and less aggressive disease (24). Therefore, we examined the immunogenicity of Tg that was an appropriate target antigen. We were able to elicit hTg-specific T cell responses using hTg-pulsed DCs suggesting the possibility of an immunotherapeutic protocol involving vaccination with DCs may be an effective approach to the problem.

DCs reportedly internalize exogenous Ags by way of the receptor-mediated endocytosis and pinocytosis (25,26); mannose-associated proteins are internalized via mannose receptors, while other glycoproteins with larger molecular weights are internalized by macropinocytosis (27,28). We found that FITC-conjugated Tg is internalized by iDCs more than mDCs in a time- and concentration-dependent manner, most likely via macropinocytosis, and then processed as an Ag. Mature DCs are differentiated from iDCs by stimulations such as TNF-α, LPS and CD40 ligand, and getting to have strong ability of antigen presentation and stimulation of T cells (29). In contrast, iDCs that express lower costimulatory molecules induce immunotolerance by acting with T cells (30). In this study, we observed that hTg-pulsed mDCs induced hTg-specific T cell responses, but hTg-pulsed iDCs did not (data not shown). This finding suggests that there is a small number of Tg-specific T cells present in peripheral

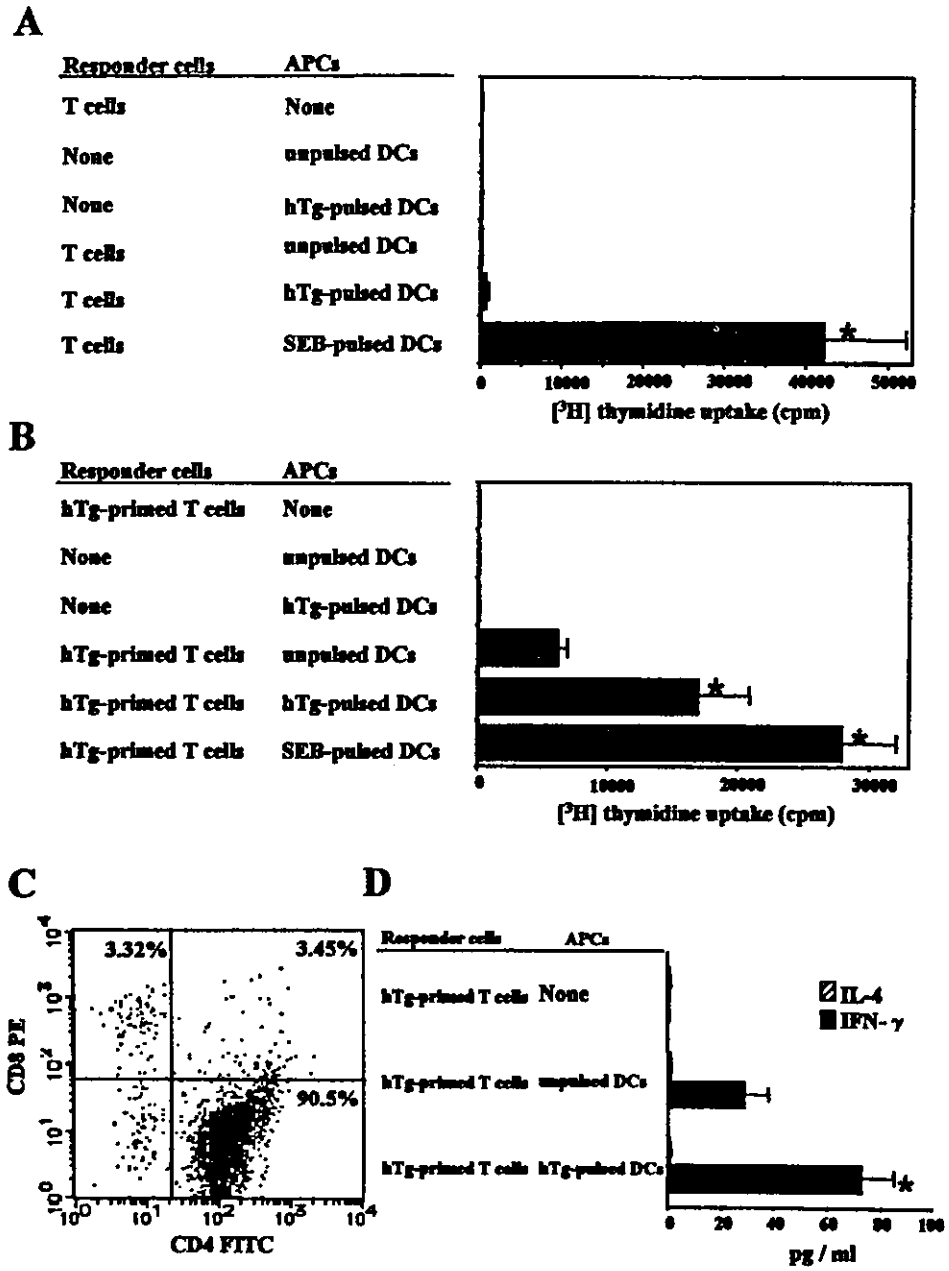

Figure 4. hTg-pulsed DCs induced hTg-specific T-cell responses. Freshly isolated T cells (A) or hTg-primed T cells (B and D) were cultured with or without unpulsed or hTg-pulsed DCs in the presence or absence of SEB, and T cell proliferation was determined by [^{3}H]-thymidine incorporation (A and B). In addition, the supernatant from each culture was assayed for IFN-γ and IL-4 using specific ELISAs (D). hTg-primed T cells were double-labeled with surface markers CD4 and CD8, and analyzed by FACS (C). Values are the means ± SD obtained for triplicate cultures. Data are representative of four individual experiments; *$p<0.05$ vs. unpulsed DC's co-culture.

blood of healthy individuals, and that these cells effectively proliferate in response to hTg-pulsed mDCs, at least *in vitro*. That implies vaccination with hTg-pulsed mDCs would induce expansion and activation of naturally occurring hTg-specific T cells, thereby enhancing anti-thyroid cancer immunity.

As shown in Fig. 4, 90% of hTg-primed T cells were CD4$^+$ cells producing IFN-γ in response to hTg-pulsed mDCs *in vitro*. This suggests that hTg-pulsed mDCs may activate hTg-specific Th1 CD4$^+$ cells. On the other hand, it is known that cytotoxic T lymphocyte (CTL) precursor also produces IFN-γ (31), which means that approximately 10% of activated hTg-responsive T cells could be IFN-γ producing hTg-specific CD8$^+$ T precursors. CD8$^+$ T cells have been implicated in anti-tumor immunity previously, and several clinical trials have been carried out with the aim of targeting MHC class I-restricted tumor antigens using CD8$^+$ T cells (6,32,33). However, the effects of CD8$^+$ cells are usually transient, and these therapies are not always successful. Much attention has recently been paid to MHC class II-restricted tumor antigens, which activate CD4$^+$ cells known to generate antitumor immunity (34). For instance, Th1 CD4$^+$ cells help to prime CD8$^+$ T cell responses (35), and in the absence of CD4$^+$ cells DCs do not activate CD8$^+$ cells, but instead induce tolerance (36). CD4$^+$ T cells also secrete cytokines (e.g., IL-2) important for

maintaining $CD8^+$ T cell effector function (37), and Th1 $CD4^+$ T cells may even induce tumor regression in the absence of $CD8^+$ cells (34,38). It is therefore possible that hTg-induced hTg-specific $CD4^+$ Th1 cells induce regression of thyroid tumors by acting in conjunction with hTg-specific $CD8^+$ T precursor cells.

For clinical applications, we examined whether autologous hTg-pulsed mDCs from advanced thyroid cancer patients actually could induce T cell activation. But hTg-primed T cells were not activated by hTg-pulsed mDCs (data not shown). We speculate the reasons as below. First, mDCs derived from advanced cancer patients are insufficient to activate immunoresponse (39). Second, recently report suggested a concept of 'semi-mature' DCs maturated by only TNF-α which did not fully function for antigen presentation and T cell activation (40), and mDCs that were used in this study were matured only by TNF-α from iDCs. Third, since serum Tg level in these advanced thyroid cancer patients is extremely high for a long time, the immunoresponse to Tg might fail into tolerance. Based on the above, we need more effective methods in a case of cancer patients to induce active immunoresponse to hTg, as was seen in healthy individuals.

Overall we found hTg could induce immune responses, although it was shown in some animal models, and hTg-pulsed mDCs may be useful for activation of hTg-specific T cells, which suggest it may be possible to develop an immunotherapeutic protocol in which hTg-pulsed mDCs are used to treat therapy-resistant thyroid cancers. More studies that confirm that hTg can induce tumor immunity in thyroid cancer patients, and more effective protocols to elicit an adaptive immunity is needed in the next step.

Acknowledgements

We thank to Dr Tsuneo A. Takahashi for helping with FACS analysis.

References

1. Mazzaferri E: Carcinoma of follicular epithelium. Radioiodine and other treatment and outcomes. In: The Thyroid. Braverman LE and Utiger RD (eds). Lippincott Williams and Wilkins, Philadelphia, pp904-929, 2000.
2. Schlumberger M and Caillou B: Carcinoma of follicular epithelium. Miscellaneous tumors. In: The Thyroid. Braverman LE and Utiger RD (eds). Lippincott Williams and Wilkins, Philadelphia, pp944-948, 2000.
3. Black EG, Sheppard MC and Hoffenberg R: Serial serum thyroglobulin measurements in the management of differentiated thyroid carcinoma. Clin Endocrinol 27: 115-120, 1987.
4. Gerfo PL, Feind C, Weber C and Ting W: Immunotherapy of thyroid cancer by induction of autoimmune thyroiditis. Surgery 94: 959-965, 1983.
5. Banchereau J and Steinman RM: Dendritic cells and the control of immunity. Nature 392: 245-252, 1998.
6. Nestle FO, Alijagic S, Gilliet M, Sun Y, Grabbe S, Dummer R, Burg G and Schadendorf D: Vaccination of melanoma patients with peptide- or tumor lysate-pulsed dendritic cells. Nat Med 4: 328-332, 1998.
7. Fong L and Engleman EG: Dendritic cells in cancer immunotherapy. Annu Rev Immunol 18: 245-273, 2000.
8. Dittel BN, Visintin I, Merchant RM and Janeway CA Jr: Presentation of the self antigen myelin basic protein by dendritic cells leads to experimental autoimmune encephalomyelitis. J Immunol 163: 32-39, 1999.
9. Ludewig B, Odermatt B, Ochsenbein AF, Zinkernagel RM and Hengartner H: Role of dendritic cells in the induction and maintenance of autoimmune diseases. Immunol Rev 169: 45-54, 1999.
10. Weetman A: Chronic autoimmune thyroiditis. In: The Thyroid. Braverman LE and Utiger RD (eds). Lippincott Williams and Wilkins, Philadelphia, pp721-732, 2000.
11. Li Volsi V: Pathology of thyroid diseases. In: The Thyroid. Braverman LE and Utiger RD (eds). Lippincott Williams and Wilkins, Philadelphia, pp488-511, 2000.
12. Volpe R: The pathology of thyroiditis. Hum Pathol 9: 429-438, 1978.
13. Vladutiu AO and Rose NR: Autoimmune murine thyroiditis relation to histocompatibility (H-2) type. Science 174: 1137-1139, 1971.
14. Esquivel PS, Rose NR and Kong YM: Induction of autoimmunity in good and poor responder mine with mouse thyroglobulin and lipopolysaccharide. J Exp Med 145: 1250-1263, 1977.
15. Creemers P, Giraldo AA, Rose NR and Kong YM: T-cell subsets in the thyroids of mice developing autoimmune thyroiditis. Cell Immunol 87: 692-697, 1984.
16. Watanabe H, Inaba M, Adachi Y, Sugiura K, Hisha H, Iguchi T, Ito T, Yasumizu R, Inaba K, Yamashita T and Ikehara S: Experimental autoimmune thyroiditis induced by thyroglobulin-pulsed dendritic cells. Autoimmunity 31: 273-282, 1999.
17. Mahnke K, Schmitt E, Bonifaz L, Enk AH and Jonuleit H: Immature, but not inactive: the tolerogenic function of immature dendritic cells. Immunol Cell Biol 80: 477-483, 2002.
18. Sato K, Nagayama H, Tadokoro K, Juji T and Takahashi TA: Extracellular signal-regulated kinase, stress-activated protein kinase/c-Jun N-terminal kinase, and $p38^{mapk}$ are involved in IL-10-mediated selective repression of TNF-α induced activation and maturation of human peripheral blood monocyte-derived dendritic cells. J Immunol 162: 3865-3872, 1999.
19. Sato K, Kawasaki H, Nagayama H, Enomoto M, Morimoto C, Tadokoro K, Juji T and Takahashi TA: TGF-ß1 reciprocally controls chemotaxis of human peripheral blood monocyte-derived dendritic cells via chemokine receptors. J Immunol 164: 2285-2295, 2000.
20. Nagayama H, Sato K, Kawasaki H, Enomoto M, Morimoto C, Tadokoro K, Juji T, Asano S and Takahashi TA: IL-12 responsiveness and expression of IL-12 receptor in human peripheral blood monocyte-derived dendritic cells. J Immunol 165: 59-66, 2000.
21. Cella M, Engering A, Pinet V, Pieters J and Lanzavecchia A: Inflammatory stimuli induce accumulation of MHC class II complexes on dendritic cells. Nature 388: 782-787, 1997.
22. Kashima K, Yokoyama S, Noguchi S, Murakami N, Yamashita H, Watanabe S, Uchino S, Toda M, Sasaki A, Daa T and Nakayama I: Chronic thyroiditis as a favorable prognostic factor in papillary thyroid carcinoma. Thyroid 8: 197-202, 1998.
23. Kebebew E, Treseler PA, Ituarte PH and Clark OH: Coexisting chronic lymphocytic thyroiditis and papillary thyroid cancer revisited. World J Surg 25: 632-637, 2001.
24. Matsubayashi S, Kawai K, Matsumoto Y, Mukuta T, Morita T, Hirai K, Matsuzuka F, Kakudoh K, Kuma K and Tamai H: The correlation between papillary thyroid carcinoma and lymphocytic infiltration in the thyroid gland. J Clin Endocrinol Metab 80: 3421-3424, 1995.
25. Steinman RM and Swanson J: The endocytic activity of dendritic cells. J Exp Med 182: 283-288, 1995.
26. Mellman I and Steinman RM: Dendritic cells: specialized and regulated antigen processing machines. Cell 106: 255-258, 2001.
27. Reis e Sousa C, Stahl PD and Austyn JM: Phagocytosis of antigens by Langerhans cells *in vitro*. J Exp Med 178: 509-519, 1993.
28. Lutz MB, Rovere P, Kleijmeer MJ, Rescigno M, Assmann CU, Oorschot VM, Geuze HJ, Trucy J, Demandolx D, Davoust J and Ricciardi-Castagnoli P: Intracellular routes and selective retention of antigens in mildly acidic cathepsin D/lysosome-associated membrane protein-1/MHC class II-positive vesicles in immature dendritic cells. J Immunol 159: 3707-3716, 1997.
29. Labeur MS, Roters B, Pers B, Mehling A, Luger TA, Schwarz T and Grabbe S: Generation of tumor immunity by bone marrow-derived dendritic cells correlates with dendritic cell maturation stage. J Immunol 162: 168-175, 1999.
30. Guermonprez P, Valladeau J, Zitvogel L, Thery C and Amigorena S: Antigen presentation and T cell stimulation by dendritic cells. Annu Rev Immunol 20: 621-667, 2002.

31. Hamann D, Baars PA, Rep MH, Hooibrink B, Kerkhof-Garde SR, Klein MR and van Lier RA: Phenotypic and functional separation of memory and effector human CD8+ T cells. J Exp Med 186: 1407-1418, 1997.
32. Rosenberg SA, Yang JC, Schwartzentruber DJ, Hwu P, Marincola FM, Topalian SL, Restifo NP, Dudley ME, Schwarz SL, Spiess PJ, Wunderlich JR, Parkhurst MR, Kawakami Y, Seipp CA, Einhorn JH and White DE: Immunologic and therapeutic evaluation of a synthetic peptide vaccine for the treatment of patients with metastatic melanoma. Nat Med 4: 321-327, 1998.
33. Marchand M, van Baren N, Weynants P, Brichard V, Dreno B, Tessier MH, Rankin E, Parmiani G, Arienti F, Humblet Y, Bourlond A, Vanwijck R, Lienard D, Beauduin M, Dietrich PY, Russo V, Kerger J, Masucci G, Jager E, De Greve J, Atzpodien J, Brasseur F, Coulie PG, van der Bruggen P and Boon T: Tumor regressions observed in patients with metastatic melanoma treated with an antigenic peptide encoded by gene MAGE-3 and presented by HLA-A1. Int J Cancer 80: 219-230, 1999.
34. Wang RF: The role of MHC class II-restricted tumor antigens and CD4+ T cells in antitumor imunity. Trends Immunol 22: 269-276, 2001.
35. Toes REM, Ossendorp F, Offringa R and Melief CJM: CD4 T cells and their role in antitumor immune responses. J Exp Med 189: 753-756, 1999.
36. Albert ML, Jegathesan M and Darnell RB: Dendritic cell maturation is required for the cross-tolerization of CD8+ T cells. Nat Immunol 2: 1010-1017, 2001.
37. Smyth MJ, Godfrey DI and Trapani JA: A fresh look at tumor immunosurveillance and immunotherapy. Nat Immunol 2: 293-299, 2001.
38. Hung K, Hayashi R, Lafond-Walker A, Lowenstein C, Pardoll D and Levitsky H: The central role of CD4+ T cells in the antitumor immune response. J Exp Med 188: 2357-2368, 1998.
39. Almand B, Clark JI, Nikitina E, van Beynen J, English NR, Knight SC, Carbone DP and Gabrilovich DI: Increased production of immature myeloid cells in cancer patients: a mechanism of immunosuppression in cancer. J Immunol 166: 678-689, 2001.
40. Lutz MB and Schuler G: Immature, semi-mature and fully mature dendritic cells: which signals induce tolerance or immunity? Trends Immunol 23: 445-449, 2002.

0013-7227/04/$15.00/0
Printed in U.S.A.

Endocrinology 145(7):3324–3330

doi: 10.1210/en.2003-1433

Differential Regulation of Cell Migration and Proliferation through Proline-Rich Tyrosine Kinase 2 in Endothelial Cells

KOICHIRO KUWABARA, TAKASHI NAKAOKA, KAORI SATO, TOSHIHIDE NISHISHITA, TERUKATSU SASAKI, AND NAOHIDE YAMASHITA

From Department of Advanced Medical Science (K.K., T.Na., K.S., T.Ni., N.Y.), The Institute of Medical Science, The University of Tokyo, Tokyo 108-8639, Japan; and Department of Biochemistry (T.S.), Cancer Research Institute, Sapporo Medical University School of Medicine, Sapporo 060-8556, Japan

Proline-rich tyrosine kinase 2 (Pyk2), a member of the focal adhesion kinase family, is thought to act as a key component in vasculogenesis and angiogenesis. Therefore, we studied the effect of mutant Pyk2 expression on the migration and proliferation in endothelial cells (ECs). Two types of mutant Pyk2 were examined by adenovirus vectors AxCA-Pyk2K457A, expressing a kinase inactive mutant, and AxCA-Pyk2Y402F, expressing a tyrosine autophosphorylation site mutant, in addition to AxCA-Pyk2, expressing wild-type Pyk2. Migration of ECs infected with AxCA-Pyk2Y402F increased to a level similar to that of ECs infected with AxCA-Pyk2. The size of effect was dependent on the amount of applied adenoviruses within the range of 3–30 multiplicity of infection. In contrast, AxCA-Pyk2K457A infection did not show any significant effect on cell migration. Western blotting showed that both phosphorylation of Pyk2 Y^{881} and association of $p130^{Cas}$ with Pyk2 were enhanced in ECs infected with AxCA-Pyk2Y402F as well as with AxCA-Pyk2, but not in ECs infected with AxCA-Pyk2K457A. Therefore, signaling mediated by Pyk2 Y^{881} and $p130^{Cas}$ may be involved in the migration of ECs infected either with AxCA-Pyk2Y402F or with AxCA-Pyk2. In proliferation assay, AxCA-Pyk2 infection suppressed EC proliferation significantly; however, neither AxCA-Pyk2Y402F nor AxCA-Pyk2K457A showed such an inhibitory effect. Thus, the two Pyk2 mutants revealed that Pyk2 signaling differentially regulates cell migration and proliferation pathways. (*Endocrinology* 145: 3324–3330, 2004)

MIGRATION AND PROLIFERATION of endothelial cells (ECs) constitute an essential part of vasculogenesis and angiogenesis. Chemokines and their receptors have been reported to play important roles in vasculogenesis and angiogenesis as well as in inflammatory responses (1). Several members of the chemokine superfamily, including stromal-derived factor-1α (SDF-1α), act as potent chemoattractants for ECs (2). CXC chemokine receptor 4 (CXCR4), a member of the G protein-coupled receptor family, is a specific receptor for SDF-1α. The expression of CXCR4 on the EC membrane is stimulated by vascular endothelial growth factor (VEGF) or basic fibroblast growth factor, both of which are well-known vasculogenic and angiogenic factors (3). Signal transduction through CXCR4 and through another type of chemokine receptor (CC-chemokine receptor 5) leads to activation of proline-rich tyrosine kinase 2 (Pyk2; also known as related adhesion focal tyrosine kinase, focal adhesion kinase 2, cell adhesion kinase β (CAKβ), or calcium-dependent tyrosin kinase), a member of the focal adhesion kinase (FAK) family (4). FAK stimulates migration of Chinese hamster ovary cells, which depends upon autophosphorylation of FAK Y^{397} (5). Upon Y^{397} autophosphorylation, Src tyrosine kinase is recruited to FAK, and the subsequent tyrosine phosphorylation of $p130^{Cas}$ is crucial in FAK-stimulated cell migration (6, 7). Although Pyk2 structurally resembles FAK, their functions are different from each other in the following points. FAK colocalizes with paxillin in the cytoplasm, and this association appears to be involved in cell migration (8). On the other hand, Pyk2 is also able to associate with paxillin, but endogenous Pyk2 does not colocalize with paxillin in the cytoplasm (9, 10). Moreover, tyrosine phosphorylation of FAK and Pyk2 is regulated differently during epithelial-mesenchymal transdifferentiation in cell migration (11) and in neuronal activation (12). From these findings, it is suggested that FAK and Pyk2 are involved in different signaling events (10). Pyk2 is implicated in multiple cellular processes such as neurotransmission (13), T and B cell signaling (14), actin-cytoskeleton organization, and cell proliferation (15). In this study, we focused on the role of Pyk2 in vasculogenesis and angiogenesis to examine the effect of two Pyk2 mutants on migration and proliferation in ECs.

Abbreviations: CAKβ, Cell adhesion kinase β; CXCR4, CXC chemokine receptor 4; EC, endothelial cell; FAK, focal adhesion kinase; hMVECs-d, human dermal microvascular endothelial cells; hUVECs, human umbilical vascular endothelial cells; MOI, multiplicity of infection; pAb, polyclonal antibody; Pyk2, proline-rich tyrosine kinase 2; RT, room temperature; SDF-1α, stromal-derived factor-1α; TBS, Tris-buffered saline; TBS-T, Tris-buffered saline with Tween 20; VEGF, vascular endothelial growth factor.

Endocrinology is published monthly by The Endocrine Society (http://www.endo-society.org), the foremost professional society serving the endocrine community.

Materials and Methods

Reagents

Anti-ERK1/2 polyclonal antibody (pAb) and antiphosphorylated ERK1/2 pAb (anti-ACTIVE MAPK pAb) were purchased from Promega Corp. (Madison, WI). Anti-$p130^{Cas}$ pAb and protein G-agarose beads were purchased from Upstate Biotechnology (Lake Placid, NY). VEGF

was purchased from R&D Systems Inc. (Minneapolis, MN). Recombinant human SDF-1α was purchased from PeproTech EC Ltd. (London, UK). Bovine albumin fraction V solution was purchased from Invitrogen Corp. (Carlsbad, CA). Enhanced chemiluminescence Western blotting detection reagents and nitrocellulose membrane (Hybond-ECL) were purchased from Amersham Biosciences UK Ltd. (Buckinghamshire, UK). Nitrocellulose transfer membrane (PROTRAN) was purchased from Schleicher & Schuell GmbH (Dassel, Germany). Anti-Pyk2/CAKβ pAb, anti-Pyk2 [pY^{402}] phosphospecific antibody, anti-Pyk2 [pY^{579}] phosphospecific antibody, anti-Pyk2 [pY^{580}] phosphospecific antibody, anti-Pyk2 [pY^{881}] phosphospecific antibody, biotin-conjugated goat F(ab')^2 antirabbit Ig, biotin-conjugated goat F(ab')^2 antimouse Ig, and streptavidin-horseradish peroxidase were purchased from Biosource International, Inc. (Camarillo, CA). Micro-BCA protein assay reagent was purchased from Pierce Biotechnology, Inc. (Rockford, IL). EBM-2 (EC basal medium), EGM-2 (EC medium), EGM-2 MV (microvascular EC medium), and GA-1000 (aqueous solution of gentamicin sulfate and amphotericin-B) were purchased from Cambrex Bio Science Walkersville, Inc. (Walkersville, MD).

Construction of Pyk2 mutants

Full-length Pyk2 cDNA was cloned into pBSSK(+) (Pyk2SK). Pyk2 has four potential phosphorylatable tyrosyl residues (Y^{402}, Y^{579}, Y^{580}, and Y^{881}). We mutated Y^{402}, an autophosphorylation site analogous to Y^{397} in FAK (16), and K^{457}, which is essential for the tyrosine kinase activity (17). Mutagenesis was performed using the Muta-Gene phagemid *in vitro* mutagenesis kit (Bio-Rad Laboratories, Inc., Hercules, CA) as described previously (18). The mutagenesis primer ATGTAGCTGTCGCGACCTGCAAGAA is specific for Y402F, a substitution of the authentic tyrosine 402 with phenylalanine; mutagenesis primer AGTCAGACATCTTTGCAGAGATTCC is specific for K457A, a substitution of the authentic lysine 457 with alanine. Pyk2 plasmid was digested with *Hpa*I and *Sca*I, and the resultant 1.3-kbp fragment was cloned into the *Eco*RV site of pBSSK(+). The orientation was checked by restriction with *Avr*II and *Eco*RI. The clone with the right orientation was then transfected into cj239 to generate uracil-containing single-stranded DNA as mutagenesis template. Mutagenesis primers were annealed to the template, followed by conversion of closed circular DNA. The mutation was confirmed by sequencing. Finally, the authentic 0.9-kbp fragment in Pyk2SK, which was restricted with *Avr*II and *Pin*AI, was replaced with the corresponding mutant fragment to obtain mutant full-length cDNA, Pyk2Y402F and Pyk2K457A, respectively.

Construction of adenoviruses AxCA-Pyk2Y402F and AxCA-Pyk2K457A

A replication-deficient adenovirus was created using the Adenovirus Kit (Takara Bio Inc., Shiga, Japan), essentially as described previously (19). The mutant cDNA containing the complete coding region of Pyk2 was blunt-ended and cloned into the *Swa*I site of a cosmid, pAxCAwt. The orientation of the insert was checked by restriction with *Bam*HI. The resulting cosmid was cotransfected to the 293 embryonic cell line with an *Eco*T221-digested DNA-terminal protein complex to generate the replication-deficient adenoviruses, AxCA-Pyk2Y402F and AxCA-Pyk2K457A. The obtained viral clones were isolated, screened for the insert, and propagated. The viruses were titrated and stocked in PBS containing 10% glycerol at −80 C. AxCA-LacZ (a replication-deficient adenovirus carrying the *Escherichia coli* β-galactosidase gene) and Ad5dlx (20), which were kindly provided by Professor Izumu Saito (Institute of Medical Science, University of Tokyo, Tokyo, Japan), and AxCA (a vector containing no foreign gene) (21), which was kindly provided by Professor Yoh Takuwa (School of Graduate Medical Science, Kanazawa University, Kanazawa, Japan), were used as negative controls. A wild-type Pyk2-expressing adenovirus vector was used as a positive control.

Cells

Human umbilical vascular ECs (hUVECs) and human dermal microvascular endothelial cells (hMVECs-d) were purchased from Bio Whittaker (San Diego, CA). hUVECs were grown in EGM-2 containing 2% fetal bovine serum, and hMVECs-d were grown in EGM-2 MV containing 5% fetal bovine serum. In the case of serum deprivation, EBM-2 supplemented with GA-1000 and 44 pmol/liter VEGF was used as basal media for both hUVECs and hMVECs-d.

Western blotting analysis

hMVECs-d uninfected or infected with adenoviruses were lysed in extraction buffer (125 mmol/liter Tris, pH 6.8; 4% sodium dodecyl sulfate, 20% glycerol, and 0.002% bromophenol blue), followed by boiling for 3 min. After adjustment for protein concentration, 2-mercaptoethanol was added to the sample (final 5%). Next, samples separated on a 4–20% gradient sodium dodecyl sulfate-polyacrylamide gel were transferred onto nitrocellulose membranes. The membranes were soaked in 10 mmol/liter Tris-HCl and 140 mmol/liter NaCl (pH 7.5) [Tris-buffered saline (TBS)] containing 4% skim milk for 2 h at room temperature (RT). The blots were incubated with the indicated primary antibody in TBS with 0.1% Tween 20 (TBS-T) at 4 C overnight. After washing in TBS-T, the blots were further incubated with biotin-conjugated secondary antibody in TBS-T containing 0.1% BSA for 2 h at RT. After the reaction with streptavidin-horseradish peroxidase in TBS-T containing 0.1% BSA for 1 h at RT, the detection was performed using enhanced chemiluminescence Western blotting detection reagents. Primary antibodies and biotin-conjugated secondary antibodies were used at recommended dilution, and streptavidin-horseradish peroxidase was used at 0.1 g/liter.

Cell migration assay

Chemotaxis assay was performed by the Boyden chamber method using a filter of 6.5-mm diameter and 8.0-mm pore size (Transwell; Corning Inc., Corning, NY) as reported by Bleul *et al.* (22). The filters were presoaked in PBS containing 0.1% gelatin for 30 min. Typically, at a confluency of 70–90%, growth media were replaced with basal media. Replication-deficient adenovirus, AxCA, AxCA-Pyk2, AxCA-Pyk2Y402F, or AxCA-Pyk2K457A, was added to the basal media at the indicated multiplicity of infection (MOI). After a 24-h incubation period at 37 C under 5% CO_2, the cells were detached by 0.025% trypsin and 0.01% EDTA, followed by centrifugation. The cell pellet was resuspended in PBS and maintained at 4 C for 2 h. Then, typically 3.0×10^5 hUVECs or hMVECs-d resuspended in 100 μl of PBS were transferred to the upper compartment of the Transwell, while the bottom well was filled with 600 μl of RPMI 1640 medium with or without 125 nmol/liter SDF-1α. The chambers were incubated for 2 h at 37 C under 5% CO_2. At the end of incubation, the upper surface of the filters was mechanically scraped off, and the filters were fixed in methanol and stained with hematoxylin and eosin to estimate the number of cells that had migrated through the pores in the filters. The stained cells were counted as the mean number of the cells per five to nine high-power fields. Each independent experiment was repeated at least twice.

Immunoprecipitation

Cells seeded on 10-cm tissue culture plates were lysed in 0.9 ml RIPA buffer (50 mmol/liter Tris-HCl, 150 mmol/liter NaCl, 1 mmol/liter EDTA, 1% Nonidet P-40, 0.25% sodium deoxycholate, pH 7.4) containing 1 mmol/liter Na_3VO_4, 10 mmol/liter $Na_4P_2O_7$, 10 mmol/liter NaF, and proteinase inhibitors (1 mmol/liter phenylmethylsulfonyl fluoride, 7 mmol/liter leupeptin, 4 mmol/liter pepstatin A, and 0.4 mmol/liter aprotinin). Phenylmethylsulfonyl fluoride was dissolved in dimethyl sulfoxide at 100 mmol/liter and added to the buffer just before use. The cell lysate was collected into a 1.5-ml tube after passing through 22-gauge needle and maintained on ice for 30 min. After microcentrifugation at $10^4 \times g$ for 10 min at 4 C, the supernatants were transferred to other tubes. To each tube, 1 μg of anti-p130^{Cas} pAb was added and incubated for 2 h at 4 C by gentle rocking. Twenty milliliters of 50% slurry of protein G-agarose beads were added, and incubation was further continued for 16 h. The beads were washed extensively in PBS and then boiled in 40 μl of extraction buffer for 3 min and subjected to Western blotting by anti-Pyk2/CAKβ pAb as described earlier.

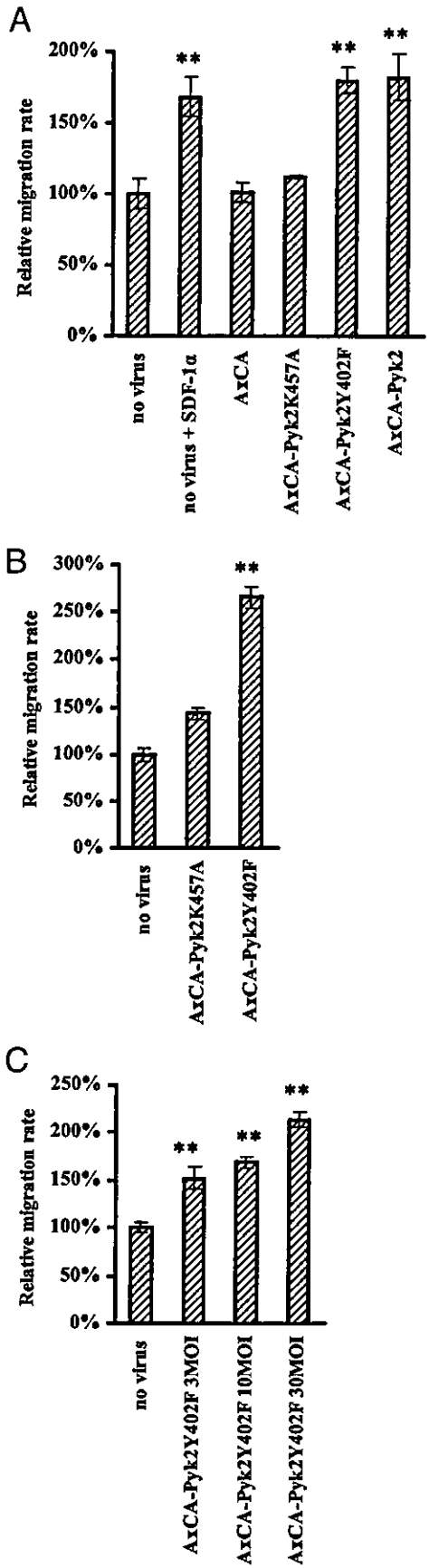

tion stimulated by AxCA-Pyk2Y402F is dependent on the infected MOI. Similar results were reproduced in two independent experiments.

Tyrosine phosphorylation of mutant Pyk2 proteins in hMVECs-d

SDF-1α and VEGF are known to stimulate EC migration vigorously (3, 24–25). To examine the involvement of four potential phosphorylatable tyrosyl residues of Pyk2 (Y^{402}, Y^{579}, Y^{580}, and Y^{881}) in EC migration, the lysates from hUVECs, stimulated either with SDF-1α or with VEGF, were subjected to Western blotting with anti-Pyk2 phosphospecific pAbs toward [pY^{402}], [pY^{881}], [pY^{579}], and [pY^{580}]. As shown in Fig. 3, the phosphorylation of Y^{402} and Y^{881} was clearly stimulated either with SDF-1α or with VEGF at 5 min; however, phosphorylation of Y^{579} and Y^{580} was not clearly detected, suggesting potential involvement of phosphorylation of Y^{402} and Y^{881}, but not of Y^{579} and Y^{580}, in the pathway stimulated by SDF-1α and VEGF.

We also subjected lysates from hMVECs-d infected with adenoviruses to Western blotting with the four kinds of anti-Pyk2 phosphospecific pAbs. The reaction of anti-Pyk2 [pY^{881}] phosphospecific pAb with lysates from hMVECs infected with AxCA-Pyk2 or AxCA-Pyk2Y402F was much greater than that with lysates from uninfected cells or cells infected with AxCA-Pyk2K457A or AxCA (Fig. 4A). Anti-Pyk2 [pY^{402}] phosphospecific pAb clearly reacted with lysates from cells infected either with AxCA-Pyk2 or with AxCA-Pyk2K457A. As expected, lysates from cells infected with AxCA-Pyk2Y402F did not react with anti-Pyk2 [pY^{402}] pAb (Fig. 4B). Neither anti-Pyk2 [pY^{579}] phosphospecific pAb nor anti-Pyk2 [pY^{580}] phosphospecific pAb clearly reacted with lysates from cells infected with AxCA-Pyk2Y402F or with AxCA-Pyk2K457A (Fig. 4, C and D). These results suggested that Y^{881} phosphorylation might be associated with an increased cell migration potential, whereas loss of Y^{402} did not affect the migration potential. Besides, the findings that

FIG. 2. A, Migration assay of hUVECs infected with wild-type or mutant Pyk2-expressing adenovirus. hUVECs were uninfected (no virus) or infected with AxCA (30 MOI), AxCA-Pyk2K457A (30 MOI), AxCA-Pyk2Y402F (30 MOI), or AxCA-Pyk2 (3 MOI), and after 24 h of serum deprivation, they were applied to cell migration assay. Uninfected hUVECs were also stimulated with 125 nmol/liter SDF-1α as positive control. Results shown are expressed as the mean and SE of relative migration rate (normalized to uninfected cells as 1.0) calculated from nine microscopic fields in each condition. **, Statistical significance compared with uninfected cells (no virus) assessed as $P < 0.01$ by the Wilcoxon rank sum test. B, Stimulatory effect of AxCA-Pyk2Y402F infection on hMVECs-d migration. hMVECs-d were uninfected (no virus) or infected with AxCA-Pyk2K457A or AxCA-Pyk2Y402F at 30 MOI. After 24-h serum deprivation, migration of the cells was examined. Results shown are expressed as the mean and SE of relative migration rate (normalized to uninfected cells as 1.0) calculated from five microscopic fields in each condition. **, Statistical significance compared with uninfected cells (no virus) assessed as $P < 0.01$ by the Wilcoxon rank sum test. C, The dependency of EC migration on the MOI of AxCA-Pyk2Y402F. hMVECs-d were uninfected (no virus) or infected with AxCA-Pyk2Y402F at the concentration of 3, 10, or 30 MOI, and after 24-h serum deprivation, migration of the cells was examined. Results shown are expressed as the mean and SE of relative migration rate (normalized to uninfected cells as 1.0) calculated from five microscopic fields in each condition. **, Statistical significance compared with uninfected cells (no virus) assessed as $P < 0.01$ by the Wilcoxon rank sum test.

Cell proliferation assay

hMVECs-d were plated in a 96-well tissue culture dish at 2.8×10^3 cells per well in 100 μl of medium. After incubation for 24–48 h at 37 C under 5% CO_2, 100 μl of medium containing the indicated amount of adenoviruses was replaced with the medium in wells, and the incubation was further continued for 72 h. Then, 10 μl of Cell Counting Kit-8 (Dojindo Laboratories Inc., Kumamoto, Japan) reagent was added to each well. After 4-h incubation at 37 C under 5% CO_2, optical density at 450 nm was determined using an ELISA reader.

Statistical analysis

The Wilcoxon rank sum test was used to evaluate the statistical significance of differences between two groups. $P < 0.05$ was considered statistically significant.

Results

Expression of mutant Pyk2 protein in hMVECs-d

In the present study, we used adenoviruses expressing wild-type Pyk2 and the following two types of Pyk2 mutants: AxCA-Pyk2K457A, expressing a kinase inactive mutant, and AxCA-Pyk2Y402F, expressing a tyrosine autophosphorylation site mutant. Expression of wild-type and mutant Pyk2 proteins was confirmed by Western blotting. Lysates from cells infected with AxCA-Pyk2, AxCA-Pyk2Y402F, and AxCA-Pyk2K457A clearly reacted with anti-Pyk2/CAKβ pAb, which reacts with the C terminus of the Pyk2 protein, whereas lysates from neither AxCA-infected cells nor uninfected cells showed detectable reactivity (Fig. 1A). The detected bands in lanes 1, 2, and 3 corresponded to 116 kDa, which is consistent with the molecular mass of Pyk2 protein.

Then we examined the effect of the Pyk2 mutants on SDF-1α-stimulated ERK1/2 activation in hMVECs-d. Phosphorylation of ERK1/2 was detected in lysates from hMVECs-d both infected with AxCA-Pyk2 and uninfected (Fig. 1B). It was, however, decreased in lysates from cells infected both with AxCA-Pyk2Y402F and with AxCA-Pyk2K457A, indicating that the two Pyk2 mutants inhibited the SDF-1α-stimulated ERK1/2 activation.

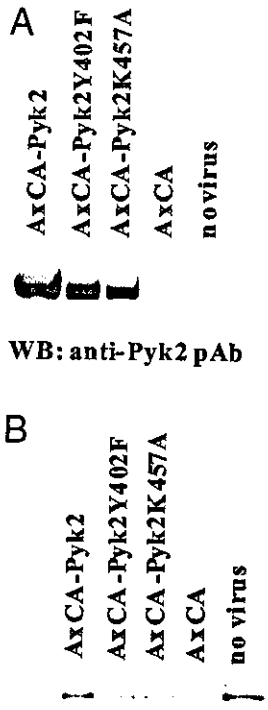

FIG. 1. A, Western blotting (WB) analysis of wild-type or mutant Pyk2 expression in hMVECs-d. hMVECs-d were uninfected (no virus) or infected with AxCA-Pyk2 (3 MOI), AxCA-Pyk2Y402F (30 MOI), AxCA-Pyk2K457A (30 MOI), or AxCA (30 MOI). After 24-h serum deprivation, the cells were lysed to subject to Western blotting with anti-Pyk2/CAKβ pAb. B, Inhibitory effect of AxCA-Pyk2Y402F or AxCA-Pyk2K457A infection on hMVECs-d ERK1/2 phosphorylation. hMVECs-d were uninfected (no virus) or infected with AxCA-Pyk2 (3 MOI), AxCA-Pyk2Y402F (30 MOI), AxCA-Pyk2K457A (30 MOI), or AxCA (30 MOI). After 24-h serum deprivation, the cells were stimulated by 12.5 nmol/liter SDF-1α in EBM-2 for 5 min and lysed to subject to Western blotting with antiphosphorylated ERK1/2 pAb (anti-ACTIVE MAPK pAb).

Pyk2Y402F increases the migration of human ECs

We examined the effects of infection either with AxCA-Pyk2Y402F or with AxCAPyk2K457A on cell migration both in hUVECs and in hMVECs-d. Figure 2A shows the representative result of migration assay in hUVECs. Compared with the control (uninfected cells), the migration of hUVECs infected with AxCA-Pyk2Y402F (30 MOI) and AxCA-Pyk2 (3 MOI) increased significantly to 180 ± 9% (mean ± SE, n = 9; $P < 0.01$) and 183 ± 16% ($P < 0.01$), respectively. The effect of infection with these constructs was similar to that of application with 125 nmol/liter SDF-1α, which increased the migration of hUVECs to 168 ± 14% ($P < 0.01$) (23). In contrast, the migration of hUVECs infected with AxCA (30 MOI) or AxCA-Pyk2K457A (30 MOI) was not different from that of the control. The migration of hUVECs infected with another control vector (Ad5dlx) was not different from that of uninfected cells (data not shown). Similar results were reproduced in two independent experiments. In the migration assay, we used AxCA-Pyk2 at 3 MOI because AxCA-Pyk2 infection at higher MOI was detrimental to hUVECs and hMVECs-d (described in *Discussion*) and because the level of Pyk2 expression in ECs infected at 3 MOI with AxCA-Pyk2 was comparable to the level of mutant Pyk2 expression in ECs infected at 30 MOI either with AxCA-Pyk2Y402F or with AxCA-Pyk2K457A.

To investigate whether the stimulation of cell migration by Pyk2Y402F was unique to hUVECs, we examined the migration of hMVECs-d. As shown in Fig. 2B, the migration of hMVECs-d infected with AxCA-Pyk2Y402F (30 MOI) increased significantly compared with control (266 ± 11%; $P < 0.01$), whereas the migration in hMVECs-d infected with AxCA-Pyk2K457A did not differ significantly from control. Similar results were reproduced in two independent experiments. Therefore, we concluded that the stimulatory effect of Pyk2Y402F on cell migration was common to both hUVECs and hMVECs-d.

Next, we examined the dependency of EC migration on the MOI of AxCA-Pyk2Y402F (Fig. 2C). The migration of hMVECs-d infected with AxCA-Pyk2Y402F was 152 ± 11% at 3 MOI, 168 ± 5% at 10 MOI, and 213 ± 8% at 30 MOI, relative to uninfected hMVECs-d. Thus, hMVECs-d migra-

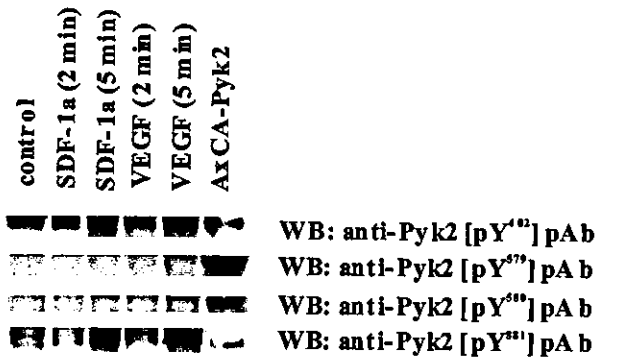

FIG. 3. Phosphorylation of Pyk2 tyrosyl residues induced by SDF-1α or VEGF in hUVECs. Lysates from hUVECs stimulated either with SDF-1α (12.5 nmol/liter) or with VEGF (2.2 nmol/liter) for 2 or 5 min were subjected to Western blotting with the following four kinds of anti-Pyk2 phosphospecific pAbs: anti-Pyk2 [pY402] pAb, anti-Pyk2 [pY579] pAb, anti-Pyk2 [pY580] pAb, and anti-Pyk2 [pY881] pAb.

FIG. 4. The effect of AxCA-Pyk2Y402F or AxCA-Pyk2K457A infection to hMVECs-d on Pyk2 tyrosine phosphorylation. hMVECs-d were uninfected (no virus) or infected with AxCA-Pyk2 (3 MOI), AxCA-Pyk2Y402F (30 MOI), AxCA-Pyk2K457A (30 MOI), or AxCA (30 MOI). After 24-h serum deprivation, the cells were lysed to react with anti-Pyk2 [pY881] phosphospecific pAb (A), anti-Pyk2 [pY402] phosphospecific pAb (B), anti-Pyk2 [pY579] phosphospecific pAb (C), or anti-Pyk2 [pY580] phosphospecific pAb (D). WB, Western blotting.

phosphorylation of neither Y^{579} nor Y^{580} was activated in AxCA-Pyk2Y402F-infected ECs, which showed high migratory potential, suggested that phosphorylation of neither Y^{579} nor Y^{580} was significantly involved in the stimulated migratory activity of ECs infected with AxCA-Pyk2Y402F.

The association of p130^{Cas} with Pyk2 in AxCA-Pyk2Y402F-infected hMVECs-d

Because activation of p130^{Cas} is implicated in FAK-mediated cell migration (8), we evaluated the association of

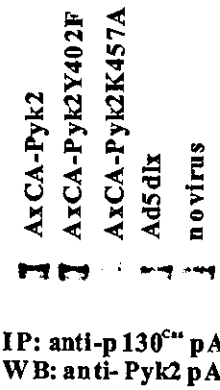

FIG. 5. Association of p130^{Cas} with Pyk2/CAKβ in hMVECs-d. The hMVECs-d were uninfected (no virus) or infected with AxCA-Pyk2 (3 MOI), AxCA-Pyk2Y402F (30 MOI), AxCA-Pyk2K457A (30 MOI), or Ad5dlx (30 MOI). After 24-h serum deprivation, each cell lysate was immunoprecipitated with anti-p130^{Cas} pAb and then immunoblotted with anti-Pyk2/CAKβ pAb. IP, Immunoprecipitation; WB, Western blotting.

p130^{Cas} with wild-type or mutant Pyk2 in hMVECs-d. Cell lysates were immunoprecipitated with anti-p130^{Cas} pAb and blotted with anti-Pyk2/CAKβ pAb. The association of p130^{Cas} with Pyk2 was more prominent in cells expressing AxCA-Pyk2 or AxCA-Pyk2Y402F when compared with uninfected cells or cells infected with AxCA-Pyk2K457A or Ad5dlx (Fig. 5). Thus, the association of p130^{Cas} with Pyk2 coincided with an increase in cell migration. The association of p130^{Cas} with Pyk2 in cells infected with AxCA-Pyk2K457A was less apparent than in uninfected cells or cells infected with Ad5dlx, suggesting that Pyk2K457A exerted some inhibitory effect on this pathway.

Proliferation of mutant Pyk2-expressing hMVECs-d

We examined the effects of infection either with AxCA-Pyk2Y402F or with AxCA-Pyk2K457A on cell proliferation in hMVECs-d (Fig. 6). AxCA-infected cells proliferated more actively than uninfected cells (138 ± 19%, n = 4; $P < 0.05$), suggesting that the infection of adenovirus vector itself might positively affect cell proliferation. AxCA-Pyk2 significantly inhibited the cell proliferation of hMVECs-d at 3 MOI (78 ± 1%; $P < 0.01$). Because AxCA-Pyk2 stimulated cell migration at 3 MOI (see Fig. 2), this inhibition was not ascribed to the cell damage caused by AxCA-Pyk2 infection. Proliferation of neither AxCA-Pyk2Y402F- nor AxCA-Pyk2K457A-infected cells (124 ± 6% and 121 ± 5%, respectively) differed significantly from that of AxCA-infected cells. Similar results were reproduced in two independent experiments. Therefore, we concluded that neither AxCA-Pyk2Y402F nor AxCA-Pyk2K457A negatively affected cell proliferation unlike AxCA-Pyk2.

Discussion

We constructed adenovirus vectors expressing a tyrosine autophosphorylation site mutant, AxCA-Pyk2Y402F, and a kinase inactive Pyk2 mutant, AxCA-Pyk2K457A. Western blotting revealed that both mutants inhibited the SDF-1α-stimulated ERK1/2 activation. Cell migration assay in hUVECs and hMVECs-d showed that overexpression of

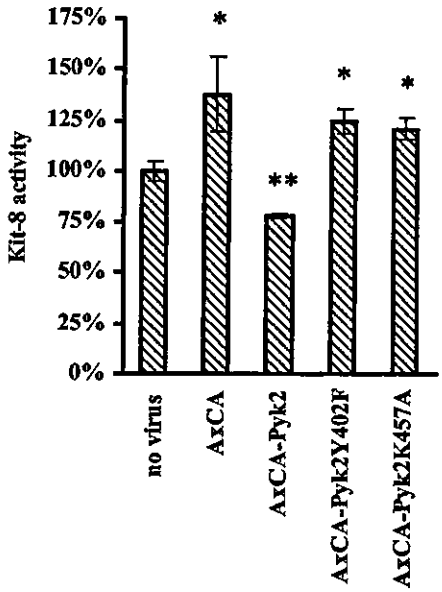

FIG. 6. Proliferation assay of hMVECs-d infected with wild-type or mutant Pyk2-expressing adenovirus. hMVECs-d were uninfected (no virus) or infected with AxCA (30 MOI), AxCA-Pyk2 (3 MOI), AxCA-Pyk2Y402F (30 MOI), or AxCA-Pyk2K457A (30 MOI) and incubated in EGM-2 MV for 72 h. Four hours after application with Kit-8 solution, the absorbance was read. Results shown are expressed as the mean and SE of relative absorbance rate (normalized to uninfected cells as 1.0) calculated from eight (uninfected cells) or four wells (infected cells) of each condition. * and **, Statistical significance compared with uninfected cells (no virus) assessed as $P < 0.05$ and $P < 0.01$ by the Wilcoxon rank sum test, respectively.

Pyk2Y402F stimulated cell migration, as did wild-type Pyk2, but that overexpression of Pyk2K457A did not affect cell migration significantly. In accordance with these results, phosphorylation of Pyk2 Y^{881} and association of $p130^{Cas}$ with Pyk2 were enhanced in hMVECs-d infected either with AxCA-Pyk2Y402F or with AxCA-Pyk2 and not in hMVECs-d infected with AxCA-Pyk2K457A. In contrast, cell proliferation assay showed that overexpression of wild-type Pyk2 suppressed cell proliferation, whereas overexpression of neither Pyk2 mutant affected cell proliferation.

Y^{402} in Pyk2 is an autophosphorylation site analogous to Y^{397} in FAK (26). Overexpression of FAK in Chinese hamster ovary cells has been shown to increase cellular migration on fibronectin (5). In this case, mutating the autophosphorylation site Y^{397} in FAK abolished its ability to stimulate cell migration, whereas overexpression of kinase-inactive FAK promoted cell migration. As opposed to those findings, our study showed that the autophosphorylation site-mutated Pyk2Y402F promoted cell migration, whereas kinase-defective Pyk2K457A did not significantly affect cell migration. Therefore, signaling through Y^{402} in Pyk2 is associated with a cellular function different from that through Y^{397} in FAK. It is noteworthy that phosphorylation status of Pyk2 was involved in increased cell migration of glioblastoma cell lines (27), suggesting that Pyk2 Y^{881} is closely involved in tumorigenesis. It might be possible that Pyk2 Y^{881} could be a molecular target of cancer therapy.

In the case of FAK, phosphorylation of Y^{397} is important for cell migration, which means that involvement of Src family kinase is essential for FAK-mediated cell migration. In contrast, EC migration did not need Pyk2 Y^{402} phosphorylation in our study, suggesting that Pyk2-mediated EC migration may not depend on Src family kinase recruitment. Phosphorylation of Pyk2 Y^{881} paralleled cell migration in our study. It is possible that Y^{881} in Pyk2Y402F was phosphorylated by natural Pyk2 itself in ECs or its activating Src family kinase. Although FAK and Pyk2 are structurally similar, they antagonize each other in certain circumstances. For example, overexpression of Pyk2 in fibroblasts leads to reorganization of cytoskeleton, which is suppressed by overexpression of FAK (15). Another study shows that FAK is required for cell survival in fibroblasts, whereas Pyk2 induces apoptosis (28). Phosphorylation of Y^{579} and Y^{580} in Pyk2 might be involved in EC migration.

It is reported that Pyk2 is abundantly expressed in pulmonary EC and plays an important role in cell migration (29). In contrast to our study, Tang *et al.* (29) showed that Pyk2Y402F did not significantly affect cell migration, whereas Pyk2K457A decreased it. This discrepancy may be attributable to the differences in experimental conditions. For example, Tang *et al.* (29) examined the effect of Pyk2 mutants on serum-stimulated cell migration, whereas we observed Pyk2Y402F-promoted cell migration in a serum-free environment. It is also possible that different EC respond to Pyk2Y402F in a different manner; in our study, overexpression of Pyk2Y402F promoted cell migration in both hMVEC-d and hUVEC, whereas Tang *et al.* (29) used pulmonary EC for their study.

A variety of extracellular signals that elevate intracellular calcium concentration and stress signals mediated by TNF-α or UV irradiation lead to activation of Pyk2 (13, 30). A model has been presented in which Pyk2 acts as bifurcation point of two signaling pathways, one leading to activation of ERK1/2 through Src recruitment and the other linking to tyrosine phosphorylation of $p130^{Cas}$ and its subsequent association with phosphatidylinositol 3-kinase (31). Pyk2 is also implicated in the c-Jun N-terminal protein kinase/stress-activated protein kinase pathway (16). In PC-12 cells, Pyk2 tyrosine phosphorylation and activation are stimulated by neuronal stimuli and stress signals, leading to the modulation of the potassium channel and activation of the c-Jun N-terminal protein kinase/stress-activated protein kinase signaling pathway, respectively (32). Our results are consistent with this model. The association of $p130^{Cas}$ with Pyk2 was detected in AxCA-Pyk2Y402F- as well as AxCA-Pyk2-infected hMVECs-d, but it was not detected in AxCA-Pyk2K457A-infected cells. Because association of $p130^{Cas}$ with Pyk2 is implicated in cell migration in several types of cells (6, 33–35), it is likely that overexpression of Pyk2Y402F promoted cell migration through association of $p130^{Cas}$ with Pyk2. It is not clear, however, what kinases are responsible for tyrosine phosphorylation of $p130^{Cas}$ in AxCA-Pyk2Y402F-infected hMVECs-d. Pyk2, Src, and Fyn tyrosine kinase are implicated in the phosphorylation of $p130^{Cas}$ dependent on the cell types (36, 37). Because no detectable bands were apparent in the control adenovirus-infected hMVECs-d in our study, association of $p130^{Cas}$ with Pyk2Y402F was not caused by a nonspecific effect of adenovirus infection.

Adenovirus-mediated overexpression of neither Pyk2Y402F

nor Pyk2K457A affected cell proliferation, whereas overexpression of wild-type Pyk2 inhibited it. Overexpression of Pyk2 has been reported to induce apoptosis (28), which is consistent with the present results. Neither of the mutations in Y^{402} nor in K^{457} inhibited EC proliferation and both of them attenuated ERK1/2 phosphorylation, suggesting that these mutations inhibited the signal transduction pathway of apoptosis induced by Pyk2. Activation of ERK1/2 occurs downstream of Src recruitment (32). It is possible that Src recruitment did not occur in ECs overexpressing the two Pyk2 mutants Pyk2Y402F and Pyk2K457A. Cell migration was stimulated not only by wild-type Pyk2 but also by Pyk2Y402F and not by Pyk2K457A, indicating that signaling through Pyk2 is involved in both cell proliferation and cell migration and that these two cellular functions are regulated through Pyk2 in different mechanisms.

Acknowledgments

We thank Professor Izumu Saito for AxCA-LacZ and Ad5dlx, and Professor Yoh Takuwa for AxCA.

Received October 23, 2003. Accepted April 2, 2004.

Address all correspondence and requests for reprints to: Naohide Yamashita, Department of Advanced Medical Science, The Institute of Medical Science, The University of Tokyo, 4-6-1, Shirokanedai, Minato-ku, Tokyo 108-8639, Japan. E-mail: yama-nao@ims.u-tokyo.ac.jp.

References

1. **Rollins BJ** 1997 Chemokines. Blood 90:909–928
2. **Gupta SK, Lysko PG, Pillarisetti K, Ohlstein E, Stadel JM** 1998 Chemokine receptors in human endothelial cells. Functional expression of CXCR4 and its transcriptional regulation by inflammatory cytokines. J Biol Chem 273:4282–4287
3. **Salcedo R, Wasserman K, Young HA, Grimm MC, Howard OM, Anver MR, Kleinman HK, Murphy WJ, Oppenheim JJ** 1999 Vascular endothelial growth factor and basic fibroblast growth factor induce expression of CXCR4 on human endothelial cells: in vivo neovascularization induced by stromal-derived factor-1α. Am J Pathol 154:1125–1135
4. **Ganju RK, Dutt P, Wu L, Newman W, Avraham H, Avraham S, Groopman JE** 1998 β-chemokine receptor CCR5 signals via the novel tyrosine kinase RAFTK. Blood 91:791–797
5. **Cary LA, Chang JF, Guan JL** 1996 Stimulation of cell migration by overexpression of focal adhesion kinase and its association with Src and Fyn. J Cell Sci 109:1787–1794
6. **Cary LA, Han DC, Polte TR, Hanks SK, Guan JL** 1998 Identification of p130Cas as a mediator of focal adhesion kinase-promoted cell migration. J Cell Biol 140:211–221
7. **Schaller MD, Hildebrand JD, Parsons JT** 1999 Complex formation with focal adhesion kinase: a mechanism to regulate activity and subcellular localization of Src kinases. Mol Biol Cell 10:3489–3505
8. **Panetti TS** 2002 Tyrosine phosphorylation of paxillin, FAK, and p130CAS: effects on cell spreading and migration. Front Biosci 7:d143–d150
9. **Sasaki H, Nagura K, Ishino M, Tobioka H, Kotani K, Sasaki T** 1995 Cloning and characterization of cell adhesion kinase β, a novel protein-tyrosine kinase of the focal adhesion kinase subfamily. J Biol Chem 270:21206–21219
10. **Schaller MD, Sasaki T** 1997 Differential signaling by the focal adhesion kinase and cell adhesion kinase β. J Biol Chem 272:25319–25325
11. **Nakamura K, Yano H, Schaefer E, Sabe H** 2001 Different modes and qualities of tyrosine phosphorylation of Fak and Pyk2 during epithelial-mesenchymal transdifferentiation and cell migration: analysis of specific phosphorylation events using site- directed antibodies. Oncogene 20:2626–2635
12. **Derkinderen P, Siciliano J, Toutant M, Girault JA** 1998 Differential regulation of FAK+ and PYK2/Cakβ, two related tyrosine kinases, in rat hippocampal slices: effects of LPA, carbachol, depolarization and hyperosmolarity. Eur J Neurosci 10:1667–1675
13. **Lev S, Moreno H, Martinez R, Canoll P, Peles E, Musacchio JM, Plowman GD, Rudy B, Schlessinger J** 1995 Protein tyrosine kinase PYK2 involved in Ca(2+)-induced regulation of ion channel and MAP kinase functions. Nature 376:737–745
14. **Berg NN, Ostergaard HL** 1997 T cell receptor engagement induces tyrosine phosphorylation of FAK and Pyk2 and their association with Lck. J Immunol 159:1753–1757
15. **Du QS, Ren XR, Xie Y, Wang Q, Mei L, Xiong WC** 2001 Inhibition of PYK2-induced actin cytoskeleton reorganization, PYK2 autophosphorylation and focal adhesion targeting by FAK. J Cell Sci 114:2977–2987
16. **Avraham H, Park SY, Schinkmann K, Avraham S** 2000 RAFTK/Pyk2-mediated cellular signalling. Cell Signal 12:123–133
17. **Sieg DJ, Ilic D, Jones KC, Damsky CH, Hunter T, Schlaepfer DD** 1998 Pyk2 and Src-family protein-tyrosine kinases compensate for the loss of FAK in fibronectin-stimulated signaling events but Pyk2 does not fully function to enhance FAK-cell migration. Embo J 17:5933–5947
18. **Nakaoka T, Kojima N, Ogita T, Tsuji S** 1995 Characterization of the phosphatidylserine-binding region of rat MARCKS (myristoylated, alanine-rich protein kinase C substrate). Its regulation through phosphorylation of serine 152. J Biol Chem 270:12147–12151
19. **Nakaoka T, Gonda K, Ogita T, Otawara-Hamamoto Y, Okabe F, Kira Y, Harii K, Miyazono K, Takuwa Y, Fujita T** 1997 Inhibition of rat vascular smooth muscle proliferation in vitro and in vivo by bone morphogenetic protein-2. J Clin Invest 100:2824–2832
20. **Saito I, Oya Y, Yamamoto K, Yuasa T, Shimojo H** 1985 Construction of nondefective adenovirus type 5 bearing a 2.8-kilobase hepatitis B virus DNA near the right end of its genome. J Virol 54:711–719
21. **Deguchi J, Namba T, Hamada H, Nakaoka T, Abe J, Sato O, Miyata T, Makuuchi M, Kurokawa K, Takuwa Y** 1999 Targeting endogenous platelet-derived growth factor B-chain by adenovirus-mediated gene transfer potently inhibits in vivo smooth muscle proliferation after arterial injury. Gene Ther 6:956–965
22. **Bleul CC, Fuhlbrigge RC, Casasnovas JM, Aiuti A, Springer TA** 1996 A highly efficacious lymphocyte chemoattractant, stromal cell-derived factor 1 (SDF-1). J Exp Med 184:1101–1109
23. **Murdoch C, Monk PN, Finn A** 1999 Cxc chemokine receptor expression on human endothelial cells. Cytokine 11:704–712
24. **Ruhrberg C** 2003 Growing and shaping the vascular tree: multiple roles for VEGF. Bioessays 25:1052–1060
25. **Mirshahi F, Pourtau J, Li H, Muraine M, Trochon V, Legrand E, Vannier J, Soria J, Vasse M, Soria C** 2000 SDF-1 activity on microvascular endothelial cells: consequences on angiogenesis in in vitro and in vivo models. Thromb Res 99:587–594
26. **Schlaepfer DD, Hauck CR, Sieg DJ** 1999 Signaling through focal adhesion kinase. Prog Biophys Mol Biol 71:435–478
27. **Lipinski CA, Tran NL, Bay C, Kloss J, McDonough WS, Beaudry C, Berens ME, Loftus JC** 2003 Differential role of proline-rich tyrosine kinase 2 and focal adhesion kinase in determining glioblastoma migration and proliferation. Mol Cancer Res 1:323–332
28. **Xiong W, Parsons JT** 1997 Induction of apoptosis after expression of PYK2, a tyrosine kinase structurally related to focal adhesion kinase. J Cell Biol 139:529–539
29. **Tang H, Hao Q, Fitzgerald T, Sasaki T, Landon EJ, Inagami T** 2002 Pyk2/CAKβ tyrosine kinase activity-mediated angiogenesis of pulmonary vascular endothelial cells. J Biol Chem 277:5441–5447
30. **Tokiwa G, Dikic I, Lev S, Schlessinger J** 1996 Activation of Pyk2 by stress signals and coupling with JNK signaling pathway. Science 273:792–794
31. **Rocic P, Govindarajan G, Sabri A, Lucchesi PA** 2001 A role for PYK2 in regulation of ERK1/2 MAP kinases and PI 3-kinase by ANG II in vascular smooth muscle. Am J Physiol Cell Physiol 280:C90–C99
32. **Dikic I, Tokiwa G, Lev S, Courtneidge SA, Schlessinger J** 1996 A role for Pyk2 and Src in linking G-protein-coupled receptors with MAP kinase activation. Nature 383:547–550
33. **Riggins RB, Quilliam LA, Bouton AH** 2003 Synergistic promotion of c-Src activation and cell migration by Cas and AND-34/BCAR3. J Biol Chem 278:28264–28273
34. **Liu B, Itoh H, Louie O, Kubota K, Kent KC** 2002 The signaling protein Rho is necessary for vascular smooth muscle migration and survival but not for proliferation. Surgery 132:317–325
35. **Klemke RL, Leng J, Molander R, Brooks PC, Vuori K, Cheresh DA** 1998 CAS/Crk coupling serves as a "molecular switch" for induction of cell migration. J Cell Biol 140:961–972
36. **Astier A, Manie SN, Avraham H, Hirai H, Law SF, Zhang Y, Golemis EA, Fu Y, Druker BJ, Haghayeghi N, Freedman AS, Avraham S** 1997 The related adhesion focal tyrosine kinase differentially phosphorylates p130Cas and the Cas-like protein, p105HEF1. J Biol Chem 272:19719–19724
37. **Sakai R, Nakamoto T, Ozawa K, Aizawa S, Hirai H** 1997 Characterization of the kinase activity essential for tyrosine phosphorylation of p130Cas in fibroblasts. Oncogene 14:1419–1426

doi:10.1016/j.ymthe.2004.07.001

Phase I Study of Autologous Tumor Vaccines Transduced with the GM-CSF Gene in Four Patients with Stage IV Renal Cell Cancer in Japan: Clinical and Immunological Findings

Kenzaburo Tani,[1,2,*] Miyuki Azuma,[3] Yukoh Nakazaki,[1,2] Naoki Oyaizu,[1] Hidenori Hase,[1] Junko Ohata,[1] Keisuke Takahashi,[1] Maki OiwaMonna,[1] Kisaburo Hanazawa,[4] Yoshiaki Wakumoto,[4] Kouji Kawai,[5] Masayuki Noguchi,[5] Yasushi Soda,[1] Reiko Kunisaki,[1] Kiyoshi Watari,[1] Satoshi Takahashi,[1] Utako Machida,[1] Noriharu Satoh,[1] Arinobu Tojo,[1] Taira Maekawa,[1] Masazumi Eriguchi,[1] Shinji Tomikawa,[1] Hideaki Tahara,[1] Yusuke Inoue,[1] Hiroki Yoshikawa,[1] Yoshitsugu Yamada,[1] Aikichi Iwamoto,[1] Hirofumi Hamada,[6] Naohide Yamashita,[1] Koh Okumura,[7] Tadao Kakizoe,[8] Hideyuki Akaza,[5] Makoto Fujime,[4] Shirley Clift,[9] Dale Ando,[9] Richard Mulligan,[10] and Shigetaka Asano[1]

[1]*Advanced Clinical Research Center, The Institute of Medical Science, University of Tokyo, Tokyo 108-8639, Japan*
[2]*Department of Advanced Molecular and Cell Therapy, Division of Molecular and Clinical Genetics, Department of Molecular Genetics, Medical Institute of Bioregulation, Kyushu University, Fukuoka 812-8582, Japan*
[4]*Department of Urology* [7]*and Department of Immunology, Juntendo University School of Medicine, Tokyo 113-8421, Japan*
[5]*Department of Urology, University of Tsukuba School of Medicine, Ibaraki 305-8575, Japan*
[3]*Department of Molecular Immunology, Division of Oral Health Sciences, Graduate School, Tokyo Medical & Dental University, Tokyo 123-8519, Japan*
[6]*Department of Molecular Medicine, Sapporo Medical University, Sapporo 060-8556, Japan*
[8]*Department of Urology, National Cancer Center Hospital, Tokyo 104-0045, Japan*
[9]*Cell Genesys, Inc., South San Francisco, CA 94080, USA*
[10]*Division of Molecular Medicine, Children's Hospital, Department of Genetics, Harvard Medical School, Boston, MA 02115, USA*

**To whom correspondence and reprint requests should be addressed at the Department of Advanced Molecular and Cell Therapy, Division of Molecular and Clinical Genetics, Department of Molecular Genetics, Medical Institute of Bioregulation, Kyushu University, 3-1-1, Maidashi, Higashi-Ku, Fukuoka-shi, Fukuoka 812-8582, Japan. Fax: 81 92 642 6444. E-mail: taniken@bioreg.kyushu-u.ac.jp.*

Available online 19 August 2004

We produced lethally irradiated retrovirally GM-CSF-transduced autologous renal tumor cell vaccines (GVAX) from six Japanese patients with stage IV renal cell cancer (RCC). Four patients received GVAX ranging from 1.4×10^8 to 3.7×10^8 cells on 6–17 occasions. Throughout a total of 48 vaccinations, there were no severe adverse events. After vaccination, DTH skin tests became positive to autologous RCC (auto-RCC) in all patients. The vaccination sites showed significant infiltration by $CD4^+$ T cells, eosinophils, and HLA-DR-positive cells. The kinetic analyses of cellular immune responses using peripheral blood lymphocytes revealed an enhanced proliferative response against auto-RCC in four patients, and cytotoxicity against auto-RCC was augmented in three patients. T cell receptor β-chain analysis revealed oligoclonal expansion of T cells in the peripheral blood, skin biopsy specimens from DTH sites, and tumors. Western blot analysis demonstrated the induction of a humoral immune response against auto-RCC. Two of the four patients are currently alive 58 and 40 months after the initial vaccination with low-dose interleukin-2. Our results suggest that GVAX substantially enhanced the antitumor cellular and humoral

1525-0016/$30.00

doi:10.1016/j.ymthe.2004.07.001

immune responses, which might have contributed to the relatively long survival times of our patients in the present study.

Key Words: GM-CSF, renal cell cancer, CD4+ T cell, CD8+ T cell, T cell repertoire

INTRODUCTION

Each year, approximately 3000 people die of renal cell cancer (RCC) in Japan [1]. Conventional treatments, such as surgery, chemotherapy, radiotherapy, and cytokine therapies, have not been established for stage IV RCC. Approximately 25% of RCC patients have metastatic disease at the time of diagnosis, and RCC sufferers have a reported 2-year survival rate of less than 20% [2]. As RCC is considered an immunogenic tumor, various types of antitumor immunotherapy have been reported that use cytokines, such as interleukin-2 (IL-2) and interferon-α; cell therapy with LAK; or nonmyeloablative stem cell transplantation. As all of these therapies have their limitations, the introduction of more specific antitumor immunotherapy with less toxicity is required [2–8].

Granulocyte–macrophage colony-stimulating factor (GM-CSF)-secreting cancer cell vaccines, which are generated from cancer cells by *ex vivo* gene transfer, have been shown to elicit tumoricidal antitumor immune responses in a variety of animal models and in human clinical trials [9–11]. Irradiated GM-CSF-secreting cancer cell vaccines are thought to induce antitumor immune responses by recruiting antigen-presenting cells, such as dendritic cells (DCs), to the site of immunization. DCs, which are the most potent immunostimulatory antigen-presenting cells, are known to activate antigen-specific $CD4^+$ and $CD8^+$ T cells, by priming them with oligopeptides that are processed from the lethally irradiated dying cancer cells. The antitumor immune reaction induced by GM-CSF-transduced tumor cells has been reviewed previously [11].

Since the initial clinical report on the use of a GM-CSF gene-transduced tumor vaccine [10], there have been a number of clinical studies applying this technology to the treatment of melanoma, renal cell carcinoma, prostate cancer, pancreatic cancer, and non-small-cell lung cancer. All of these clinical studies were performed without any severe adverse events [12–22]. In a clinical study examining RCC, Simons *et al.* reported a randomized, double-blind dose-escalation study with equivalent doses of autologous, irradiated RCC vaccine cells, with or without *ex vivo* human GM-CSF gene transfer. GM-CSF gene-transduced vaccines were equivalent in toxicity to nontransduced vaccines up to the feasible limits of autologous tumor vaccine yield. There was no dose-limiting toxicity, no evidence of autoimmune disease, and no replication-competent retrovirus encountered in 18 patients receiving full follow-up care. This phase I study demonstrated the feasibility, safety, and bioactivity of autologous GM-CSF gene-transduced tumor vaccines for RCC patients. An objective partial response was observed in one of the three patients who received 1.2×10^8 GM-CSF gene-transduced cells and showed the largest delayed-type hypersensitivity (DTH) conversion [13,14]. However, the optimum number of GM-CSF-transduced autologous renal tumor cell vaccine (GVAX) cells for use in vaccination and boosting and the optimum frequency of cell administration remain to be determined.

To determine more precisely whether GM-CSF-secreting RCC vaccines can be used safely to induce antitumor immunity in advanced RCC patients, we conducted a clinical trial of this treatment strategy. Our clinical protocol consisted of tumor resection by nephrectomy, the establishment of primary RCC cultures, and *ex vivo* gene transfer, which was carried out in our own cell-processing facility [23]. The minimum dosage of the vaccine cells was set according to the previous report on RCC by Simons *et al.* [14], and the booster schedule was based on a previous report on non-small-cell lung cancer by Soiffer *et al.* [16]. This was the first clinical trial of human gene therapy for cancer patients approved by the Japanese government and performed in Japan. The results of the present study indicate that this novel RCC immunotherapeutic regimen, which features vaccination with GM-CSF-secreting, irradiated autologous RCC tumor cells, is feasible, safe, and capable of eliciting systemic immune responses against RCC tumor cells. Furthermore, these patients, some of whom also received systemic low-dose IL-2 therapy, have been followed up on an outpatient basis.

RESULTS

Case Presentations

Forty patients suffering from either primary RCC with or without metastases or postoperative relapsed RCC were evaluated at our hospital between July 1998 and March 2001. Of these, 6 preoperative patients with stage IV RCC (UICC classification 1997) with metastatic lesions were allowed to participate in the present clinical study by our ethics committee, based on clinical condition and eligibility criteria listed under Patients and Methods. As

TABLE 1: Patient characteristics and clinical response to GVAX

	Patient			
	1	2	3	4
Age (years)/sex	60/male	71/male	57/female	50/male
Tumor site				
Primary	Right RCC	Right RCC	Left RCC	Left RCC
Metastases	Lung, liver	Sacral bone	Liver, lung	Lung
Previous therapy	None	Sacral irradiation	None	None
GM-CSF production[a] (ng/10^6 cells/24 h)	49	98	51	116
No. of GVAX treatments	10	17	15	6
Vaccinated total cell number	2.2×10^8	3.7×10^8	3.2×10^8	1.4×10^8
Adverse events				
Systemic	Low-grade fever	Low-grade fever	None	None
Local	Erythema, pruritis	Erythema, pruritis	Erythema, pruritis	Erythema, pruritis, blister
Eosinophil number[b] (/μl; mean ± SD)	718 ± 76	437 ± 306	226 ± 283	390 ± 150
Clinical response	PD	SD	PD	PD, MR
Survival (months from first vaccination)	7.5[c]	>62	45[c]	>44

PD, progressive disease; SD, stable disease; MR, mixed response.

[a] GM-CSF production rate from each autologous GM-CSF-transduced RCC.

[b] Eosinophil number was measured 48 h after vaccination.

[c] Patient passed away.

2 patients, a 48-year-old Japanese man having right RCC with multiple lung metastases and a 58-year-old Japanese man having right RCC with metastases to the right clavicle, bilateral lung, and liver, were excluded from this study because their GM-CSF-transduced RCC cells did not produce enough GM-CSF to satisfy the eligibility criteria as described under Autologous Vaccine Yield and Gene Transfer, 4 patients received GVAX.

The first patient (Case 1), a 60-year-old Japanese man, was diagnosed in August 1998 with RCC of the right kidney with multiple lung and liver metastases. His largest metastatic tumor, which was located in the right hilar region, was calculated volumetrically as 135 ml by computed tomography (CT) scan. The vaccine preparation used, his clinical course, and the autopsy findings have been reported previously [24]. Furthermore, he received a total of 2.2×10^8 GVAX cells over 10 subcutaneous injections. The adverse events he experienced during vaccination are summarized in Table 1. He received gamma knife irradiation for his brain metastases and was initiated with low-dose (700,000–140,000 IU) recombinant IL-2 (rIL-2; Imunace, 350,000 IU/vial; Shionogi, Osaka, Japan), which was administered intravenously according to the patient's request. One week after the start of the rIL-2 treatment, the patient's right hilar mass lesion became smaller and decreased by 30% of the total volume within 1 month (Fig. 1A). Unfortunately, this patient died of multiple RCC metastases on July 8, 1999, 10 months after nephrectomy and 7 months after the start of GVAX vaccination (Fig. 2A).

The second patient (Case 2), a 71-year-old Japanese man, was diagnosed in December 1998 with a sacral tumor that metastasized from RCC of the right kidney. He received a total dose of 30 Gy of irradiation of the sacral metastasis in February 1999 for severe pain, which was followed up with spinal anesthesia and oral morphine sulfate. The patient was nephrectomized on April 6, 1999, 43 days after the local irradiation, and pathology showed clear cell carcinoma. He received a total of 3.7×10^8 GVAX cells in 17 subcutaneous injections from June 3, 1999, to February 3, 2000. The adverse events he experienced during vaccination are summarized in Table 1. His pain at the sacral area disappeared completely after the 5th vaccination, and oral morphine sulfate was discontinued. He experienced mechanical ileus due to nephrectomy after the 13th vaccination, which resolved after a few days of iv fluid treatment. The ileus was not related to the vaccination, and no recurrence of the ileus was noted after 4 further vaccinations. During the course of vaccination, the growth rate of the sacral tumor was stable as assessed by CT scan. His clinical course with the change in tumor size is described in Fig. 2B. The serum level of the nonspecific tumor marker immunosuppressive acidic protein returned from double the normal level to normal after the 6th vaccination, and a thallium scan showed decreased uptake of thallium at the tumor site on completion of the vaccination protocol (data not shown). Eleven months after the start of vaccination, pathological examination of the biopsied sacral bone specimen showed no RCC. This patient had been doing well without any treatment, with a performance status of zero, until he experienced a dull pain in his right femoral area in late November of 2001, 29 months after the 1st vaccination. He was diagnosed as having a 1-cm lytic metastasis in the right femoral bone. He received local

doi:10.1016/j.ymthe.2004.07.001

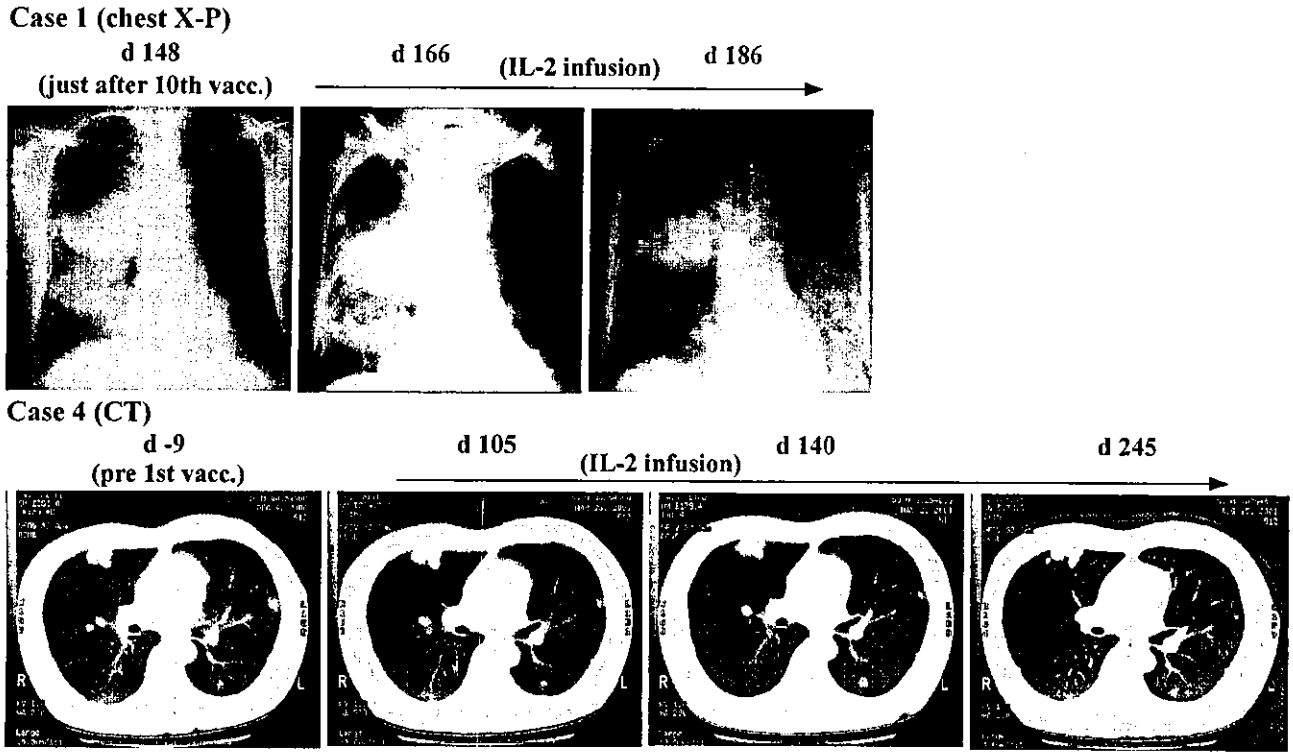

FIG. 1. Size change of the lung metastases in Cases 1 and 4 during the observation period after GVAX vaccination. (A) In Case 1, the size of the right hilar tumor, the largest metastatic lesion, became smaller after 1 week of low-dose IL-2 (d 166, day 166) and decreased by 30% after 1 month of low-dose IL-2 compared with the tumor just after the 10th vaccination. Chest X-ray films are presented. (B) In Case 4, the size of the left lung metastasis became smaller during vaccination as shown on two films for comparison between prevaccination and 105 days after the 1st vaccination. After the start of low-dose IL-2 between days 105 and 245, both the metastatic lesions in the left lung and those in the right lung became smaller. CT scan films are presented.

irradiation at a dose of 30 Gy to his femoral metastasis followed by daily low-dose rIL-2 (700,000–140,000 IU). His performance status at present, 58 months after the start of vaccination and with low-dose rIL-2 (350,000 IU) treatment, is zero.

The third patient (Case 3), a 57-year-old Japanese woman, was diagnosed in October of 1999 with RCC of the left kidney with multiple liver and lung metastases. She was nephrectomized on December 9, 1999, and the pathology showed clear cell carcinoma. She received a total of 3.2×10^8 GVAX cells in 15 subcutaneous injections, from February 22, 2000, to September 19, 2000. The adverse events she experienced during vaccination are summarized in Table 1. During the course of vaccination, the growth rate of the multiple liver tumors slowed, but the numbers and sizes of the masses did not decrease as assessed by CT scan (Fig. 2C). The sizes of the metastases in her right renal pelvis and lungs, observed on CT scan, were stable during vaccination. Her performance status was maintained at zero. After completion of the vaccination regimen, she requested systemic rIL-2 and interferon-α, but the cytokine treatments were discontinued due to the appearance of liver dysfunction, which resolved after discontinuation of cytokines. Thereafter, she received monthly LAK (lymphokine-activated killer cells) therapy, upon her request. However, her metastatic lesions gradually increased, and she ultimately died of multiple RCC metastases on November 3, 2003, 47 months after nephrectomy and 45 months after the start of GVAX vaccination.

The fourth patient (Case 4), a 50-year-old Japanese man, was diagnosed in July of 2000 with right RCC with multiple lung metastases. He was nephrectomized on September 20, 2000, and pathology showed clear cell carcinoma. He received a total of 1.4×10^8 GVAX cells in six subcutaneous injections from December 13, 2000, to February 20, 2001. The adverse events he experienced during vaccination are summarized in Table 1. During the course of vaccination, the growth rate of the largest lung tumor slowed, and several tumors disappeared or were reduced in size, i.e., a mixed response was obtained. However, the sum of all the masses was increased, as assessed by CT scan. After the sixth injection, he was found to have a metastatic brain lesion with a maximum diameter of 1 cm, and the vaccination was discontinued according to our eligibility criteria. He received gamma knife irradiation to his brain metastasis and low-dose rIL-2 (700,000–140,000 IU) was initiated, which was given

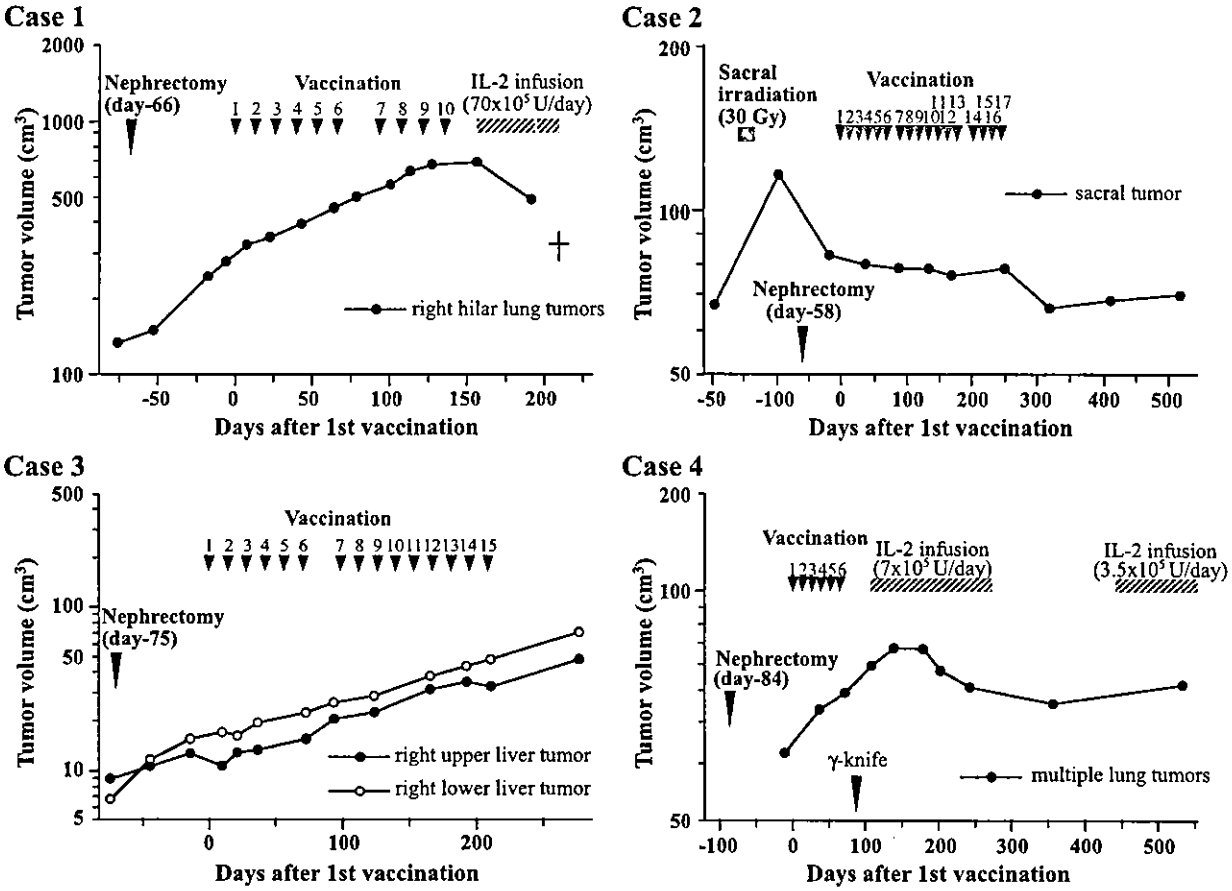

FIG. 2. Clinical summary of the four stage IV RCC patients (Cases 1 to 4) who received GVAX. The days of each vaccination are indicated by the short arrows, and the upper numbers signify the number of vaccinations. The long arrow indicates the time of nephrectomy of an RCC that involved the kidney. The tumor volume of each target metastatic lesion was measured periodically by CT scan or MRI. In Cases 1 and 4, low-dose IL-2 was administered after vaccination, upon request by the patients. The sacrum and brain were irradiated in Cases 2 and 4, respectively, to control sacral pain and brain edema.

subcutaneously, according to the patient's request. One month after the start of the rIL-2 treatment, the patient's total lung tumor volume was reduced and decreased to 30% of the peak volume over 3 months (Figs. 1B and 2D). His metastatic brain tumor was resected in January of 2002, and his performance status at present, 40 months after the start of vaccination and with low-dose rIL-2 (350,000 IU) treatment, is zero.

Autologous Vaccine Yield and Gene Transfer

In this trial, we generated the primary RCC cultures from large, advanced cancers with some areas of necrosis. The rate of successful vaccine cell expansion was 100% (6/6). In our preclinical models, the expression of paracrine GM-CSF by vaccine cells at levels higher than 40 ng/10^6 cells/24 h induced antitumor immunity, and thus, we excluded cases producing less than this level from the present study [13,14]. A single transduction with MFGS-GM-CSF generated GM-CSF secretion levels of >40 ng/10^6 cells/24 h in four of the six patients (66.6%) and their production levels are shown in Table 1. The level of GM-CSF secretion by nontransduced cells ranged from 0 to 19 ng/10^6 cells/24 h. We excluded two of the patients, who had GVAX production of only 20 and 12.4 ng/10^6 cells/24 h, respectively, from our study. Cells from these individuals incorporated fewer copies of the integrated GM-CSF cDNA, and the cell doubling times were approximately two times greater than those of the cells producing >40 ng/10^6 cells/24 h GM-CSF (data not shown). It is likely that the extended cell doubling times resulted in poor GM-CSF transduction efficiency in the two excluded cases.

Safety of Administration and Systemic Toxicities

All of the six patients' primary cultures met the vaccine cell yield specifications for at least six injections. Importantly, the tests for microbial contaminants gave negative results for all six GM-CSF-transduced products. All four patients, designated Cases 1, 2, 3, and 4, satisfied all of the eligibility criteria for this study and

doi:10.1016/j.ymthe.2004.07.001

received vaccinations (Table 1). No surgical complications were encountered that would preclude subsequent vaccination, although Case 1 had mechanical ileus 30 days after nephrectomy, which was before vaccination, and Case 2 had ileus 219 days after nephrectomy, between the 12th and the 13th vaccine injections. These symptoms were resolved by intravenous fluid replacement for several days. In the latter case, ileus was thought to be a late adverse event related to nephrectomy, but not vaccination because reinitiation of vaccination did not cause any other ileus symptoms. When vaccine yield and clinical status permitted, we performed multiple vaccinations for analysis of cumulative side effects. Cases 1, 2, 3, and 4 received GVAX at 66, 58, 75, and 84 days after nephrectomy, respectively. They received 48 fully evaluable, 14-day treatment cycles. Finally, Cases 1, 2, 3, and 4 received total cell doses of 2.2×10^8, 3.7×10^8, 3.2×10^8, and 1.4×10^8, respectively. During the vaccinations, we observed no hepatic, renal, pulmonary, cardiac, neurological, or gastrointestinal toxicities in any of the patients other than mechanical ileus in Case 2 as stated above. We observed significant increases in the numbers of peripheral blood eosinophils, but not other leukocytes, after immunization, as shown in Table 1, and the peak eosinophil level gradually increased in each case after repetitive vaccinations (data not shown). We did not observe the two most concerning toxicities, vaccine site-specific ulceration and development of acute autoimmune disease and, specifically, nephritis in uninephric patients, except in Case 4, who experienced blister formation at the vaccination site following the 6th vaccination (Table 1). We detected no RCR (replication-competent retrovirus) during the postvaccination follow-up period in any of the four patients who received the vaccine cells. The apparent lack of acute, systemic toxicity in this trial was paralleled by the lack of plasma elevation of GM-CSF in pharmacokinetic studies following treatment (data not shown). Follow-up observations for long-term toxicity, including autoimmune disease, have been under way on our two surviving patients, Cases 2 and 4, and no vaccine-related long-term toxicity has been noted to date.

Phenotype of Cells at the Sites of Vaccination

Although there was some individual variation, we noted significant infiltration by $CD4^+$ T cells and eosinophils by day 30 (after the third vaccination); Case 3 had modest eosinophilic but intense mononuclear cell infiltration throughout the course of the vaccination protocol. Thereafter, these cell infiltrations were reduced in Cases 1 and 4, but increased in Cases 2 and 3. We could detect $CD68^+$ macrophages and CD20cy-positive B cells as minor populations, but their levels were unaltered during the course of the vaccination protocol. The level of HLA-DR expression by infiltrating cells was initially low, but increased by day 30. Intradermal $S100^+$ dendritic cells were occasionally observed in most cases. These findings were comparable with previous reports [14–20].

Delayed-Type Hypersensitivity Reactions

DTH tests using Multitest CMI showed that Cases 1 and 3 had anergic scores and Cases 2 and 4 had normal scores, i.e., within the range seen for normal volunteers or patients with localized cancer (data not shown). As shown in Table 2, we did not observe significant DTH reactions (>10 mm) to unpassaged, irradiated autologous RCC cells in any of the four patients prior to treatment. Following vaccination, we observed significant DTH reactions in all patients and they were strongest after the sixth vaccination. We also observed DTH reactions to normal renal cells (NRCs), but these reactions were almost always smaller than those to RCC cells.

We examined pathological phenotypes and numerical analysis of the DTH reactions. In all four cases, significant DTH reactions against RCC were induced by days 24–28 (following the second vaccination), compared with the day 0 controls (prevaccination). $CD4^+$ T cells were more dominant than $CD8^+$ T cells at the sites of DTH reaction, followed by $CD68^+$ macrophages and a few B cells, which was a common feature of DTH in all cases. We also observed various degrees of eosinophilic infiltration with degranulation. There were no significant differences between RCC and NRC with regard to the phenotypes of the cells in the DTH reaction, although more intense cell infiltration was observed against RCC than against NRC (data not shown). Although we detected significant DTH reactions until day 133 in Case 1, we observed a certain degree of attenuation in other cases.

Immunophenotypic Analysis of Tumor-Infiltrating Lymphocytes (TILs)

We performed immunophenotypic analysis of TILs for Case 1. Immunohistochemical analysis revealed that $CD4^+$ T cells were the predominant infiltrating cell type in pretherapy primary tumors, followed by B cells (data not shown). Fig. 3 shows TILs in perivascular areas (Fig. 3A), around the foci of tumor cell apoptosis (Figs. 3B and D), and in an unremarkable area (Fig. 3D), within biopsied skin metastatic RCC specimens that were obtained 5 months after initiation of therapy. Regardless of the area under observation, the T cells in this specimen were $CD8^+$, and we detected virtually no B cells. In addition, we observed increased numbers of $CD68^+$ macrophages, especially around the apoptotic foci. In contrast to the results of the DTH test, we did not observe eosinophilic infiltration of the tumors (data not shown). Interestingly, immunophenotypic analysis of the infiltrating cells at the sites of surgically resected renal cancer and normal renal tissue, autopsied normal liver, lung, and kidney showed a predominance of

TABLE 2: Immunological findings in patients who received GVAX

	Patient 1	2	3	4
Response to DTH skin test (mm)[a]				
Prevaccination	7 × 7/6 × 4.5	0 × 0/4 × 2	3 × 6/2 × 6	0 × 0/2 × 2
Peak reaction	85 × 65/30 × 35 (6)[b]	15 × 15/10 × 10 (6)[b]	25 × 25/2 × 1 (9)[b]	17 × 11/22 × 18 (6)[b]
Lymphocyte proliferation (cpm)				
Prevaccination	5,513	5,385	1402	1550
Post third	11,637	16,486	2836	6084
Post sixth	15,845	40,578	2442	6445
Cytokine production (pg/ml)				
IFN-γ				
Prevaccination	2746	UD	50	102
Post third	4952	199	481	UD
Post sixth	3568	394	967	UD
IL-5				
Prevaccination	UD	UD	395	128
Post third	1124	UD	863	1331
Post sixth	2088	792	1850	3017
IL-10				
Prevaccination	170	UD	UD	UD
Post third	80	UD	43	254
Post sixth	235	155	130	297
Cytotoxicity assay (%)				
Prevaccination	62.8	0.2	16.0	13.0
Post third	51.4	17.0	52.9	21.0
Post sixth	45.3	27.3	36.8	27.5
TCR Vβ gene-segment repertoire analysis	PB: 9,14,15,17 TIL: 10,17,21 DTH: 10,17	PB: 1,7,10,11,21 DTH: 1	PB: 4,18 DTH and Vac: 4,7	PB: 21,23 Vac: 9 DTH: 21

UD, under the detection level; PB, peripheral blood; TIL, tumor infiltrating lymphocytes; DTH, delayed type hypersensitivity.

[a] DTH reactions were examined using cultured autologous RCC cells/normal renal cells as antigens.

[b] The numbers in parentheses show that peak DTH reactions were observed after sixth or ninth vaccination.

$CD4^+$ cells, whereas analysis at the sites of biopsied or autopsied tumor tissues obtained after vaccination or after vaccination followed by low-dose IL-2, respectively, showed a predominance of $CD8^+$ cells (data not shown).

Vaccination Enhances the Proliferative Responses and Cytokine Production Against Autologous Tumors

We assessed the cellular immune responses using the peripheral blood mononuclear cells (PBMC) of patients who received GVAX. PBMC proliferated well in response to autologous RCC cell stimulation at all times tested (Table 2). In Case 2, the proliferative response observed before vaccination was augmented after vaccination. In all cases, vaccination markedly enhanced the proliferative responses to autologous RCC in the presence of IL-2. Especially, in Cases 2 and 4, those with prolonged clinically stable disease, the proliferative responses against autologous tumor cells remained high until the end of the study (data not shown).

IFN-γ in cultures stimulated with autologous RCC was enhanced after the initial vaccinations in Cases 1, 2, and 3, but not in Case 4 (Table 2). Conversely, IL-5 and IL-10 production was enhanced after vaccination in all cases. The enhancement of IL-5 seemed to correlate with the eosinophilia observed after the sixth vaccination. We also measured IL-4 production, but the levels of this cytokine were all below the limits of detection (data not shown).

Vaccination Induces Cytotoxicity Against Autologous RCC, Allogeneic RCC, and Autologous NRC

Case 1 showed comparatively high cytotoxicity against autologous RCC before vaccination. This level was maintained until after the fifth vaccination, after which it decreased. This was consistent with the higher DTH responses against autologous RCC and NRC seen in this case (Table 2). In Cases 2, 3, and 4, vaccination increased and maintained cytotoxicity against autologous RCC (Table 2, Fig. 4). Moreover, the addition of F(ab′)2 anti-CD3 mAb efficiently inhibited cytotoxicity against autologous RCC, suggesting the involvement

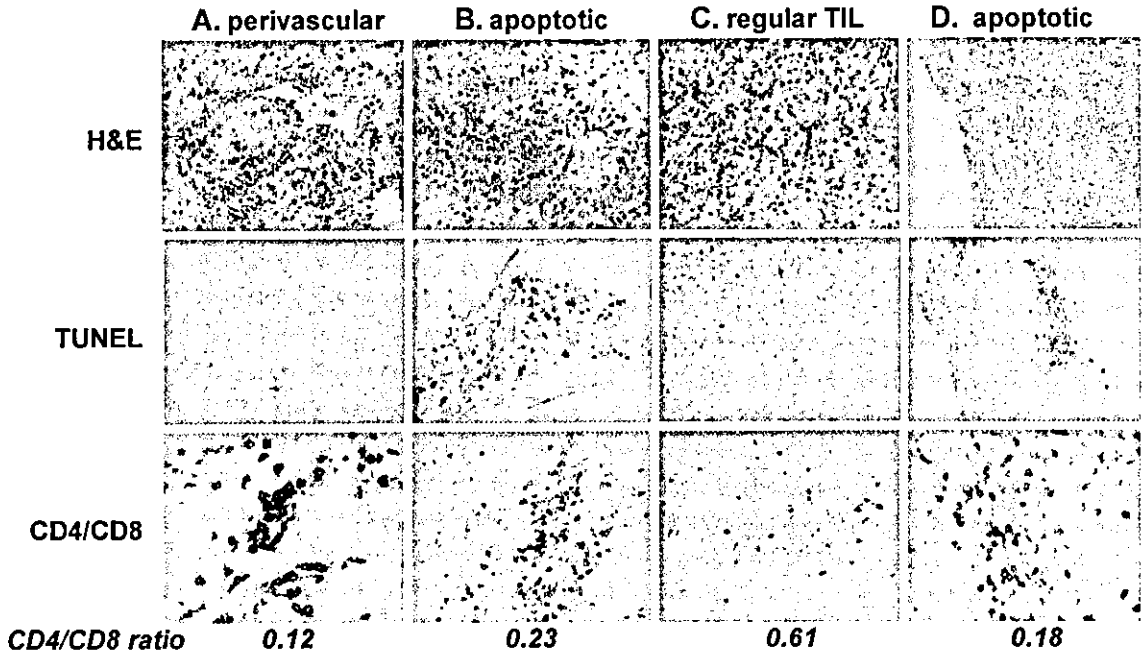

FIG. 3. Immunophenotypic analysis of tumor-infiltrating lymphocytes (TILs) in the RCC tumors of Case 1. TILs were observed in various areas, particularly (A) in the perivascular area, (B, D) around foci of tumor cell apoptosis, and (C) in unremarkable areas, within metastatic RCC that were obtained 7 months after the initiation of therapy. The T cell phenotype in this specimen had been converted to CD8 dominant, and few B cells were detected. To detect tumor apoptosis, the TUNEL method was applied as described under Patients and Methods.

FIG. 4. Cytotoxicity against autologous RCC in Cases 1 to 4. PBMC were cultured with irradiated GM-CSF-transduced autologous RCC in the presence of IL-2 for 7 days in 96-well microplates and ^{51}Cr-labeled target cells were added. After a 6-h incubation, cytotoxicity was measured as described under Patients and Methods. Asterisks in the panels for auto-RCC targets show the cytotoxicity, which was inhibited by more than 25% by the addition of F(ab')2 anti-CD3 mAb. Additional experimental values (squares) assessing the long-term results with additional treatment after the last vaccinations are also shown. IL-2, the rectangular bar represents the period of the administration of low-dose IL-2; R; γ-knife, gamma knife treatment was done for brain metastasis before the administration of IL-2.